

1. Reply to Referee#2' comments:

Thank you very much for your valuable comments and suggestions. We have gone throughout the entire manuscript sentence by sentence with the help of native speakers. Answers were shown below.

Reviewer #2: Unknown sources of HONO are one of important open questions for atmospheric chemistry. The authors analyzed thirteen datasets in literature and proposed the formula linking the flux of unknown HONO emission sources with other variables significantly correlated. They then incorporated the function into the WRF-chem model. The modeling results of HONO and free radicals were compared with those absent of the unknown sources in various zones in China. The study is indeed interesting and will significantly improve understandings of the impacts of unknown HONO emissions on atmospheric chemistry. This reviewer strongly believes that the work is worthy of publishing in ACP. The major drawback is related to technical writings and this can be done by language editing in the next round submission. This reviewer just lists a few of them which are very confusing and need to be clarified. The list is of course incomplete and the authors should work with native speakers to go throughout the entire manuscript sentence by sentence.

Specific comments:

1) The title is not readable. In the context, there are at least two unknown sources for daytime HONO. Why is it “an unknown daytime nitrous acid source...”? The authors were using mixing ratio rather than mass concentration in the context, the title should be consistent with their results. “Those” represents what? Unknown source or other? What does it mean “coastal regions”? To this reviewer, the coastal region is very small and should be within 10-50 km range from seas.

The title was revised: “Impacts of an unknown daytime HONO source on the mixing ratio and budget of HONO, and hydroxyl, hydroperoxyl and organic peroxy radicals, in the coastal regions of China”

2) Abstract, lines 13-16 and lines 18-20, the definitions of unknown sources are inconsistent and very confusing. This had to be clarified.

The description in the abstract section was revised: “Many field experiments have found high nitrous acid (HONO) mixing ratios in both urban and rural areas during daytime, but these high daytime HONO mixing ratios cannot be explained well by gas-phase production, HONO emissions, and nighttime hydrolysis conversion of

nitrogen dioxide (NO_2) on aerosols, suggesting that an unknown daytime HONO source (P_{unknown}) could exist. The formula $P_{\text{unknown}} \approx 19.60 \times \text{NO}_2 \times \text{J}(\text{NO}_2)$ was obtained using observed data from 13 field experiments across the globe. The three additional HONO sources (i.e., the P_{unknown} , nighttime hydrolysis conversion of NO_2 on aerosols, and HONO emissions) were coupled into the WRF-Chem model (Weather Research and Forecasting model coupled with Chemistry) to assess the P_{unknown} impacts on the concentrations and budgets of HONO and peroxy (hydroxyl, hydroperoxyl, and organic peroxy) radicals (RO_x) ($= \text{OH} + \text{HO}_2 + \text{RO}_2$) in the coastal regions of China.”

3) Abstract lines 25-27, “elevated” relative to what?

We used “High” instead of “Elevated”.

4) Abstracts, lines 20-36, the reviewer can guess the impact of additional HONO sources and the impact of P_{unknown} . From lines 36-50, the presentations are very confusing and need to be clarified what are impacts of additional sources and what are impacts of P_{unknown} .

The description in the abstract section was revised: “The daytime average OH production rate was enhanced by 0.67 due to the three additional HONO sources [0.64 due to the P_{unknown}] to 4.32 [3.86] ppb h^{-1} via the reaction of $\text{HO}_2 + \text{NO}$, and by 0.49 [0.47] to 1.86 [1.86] ppb h^{-1} via the photolysis of HONO, and the OH daytime average loss rate was enhanced by 0.58 [0.55] to 2.03 [1.92] ppb h^{-1} via the reaction of $\text{OH} + \text{NO}_2$ and by 0.31 [0.28] to 1.78 [1.64] ppb h^{-1} via the reaction of $\text{OH} + \text{CO}$ (carbon monoxide) in Beijing, Shanghai and Guangzhou. Similarly, the three additional HONO sources produced an increase of 0.31 [corresponding P_{unknown} contribution of 0.28] to 1.78 [1.64] ppb h^{-1} via the reaction of $\text{OH} + \text{CO}$ and 0.10 [0.09] to 0.63 [0.59] ppb h^{-1} via the reaction of CH_3O_2 [methylperoxy radical] + NO in the daytime average HO_2 production rate, and 0.67 [0.61] to 4.32 [4.27] ppb h^{-1} via the reaction of $\text{HO}_2 + \text{NO}$ in the daytime average HO_2 loss rate in Beijing, Shanghai and Guangzhou. The above results suggest that the P_{unknown} considerably enhanced the RO_x concentrations and accelerated RO_x cycles in the

coastal regions of China, and could produce significant increases in concentrations of inorganic aerosols and secondary organic aerosols and further aggravate haze events in these regions.”

5) Lines 73-75, “higher” than what?

We deleted the “higher” and the revision was made in the introduction section:

“However, many field experiments have found daytime HONO mixing ratios that are unexpectedly higher than the theoretical steady value (~10 ppt), in both urban and rural areas: e.g., 0.15–1.50 ppb in Asia (Su et al., 2008; Wu et al., 2013; Spataro et al., 2013), 0.01–0.43 ppb in Europe (Kleffmann et al., 2005; Acker et al., 2007; Sörgel et al., 2011; Michoud et al., 2014), 0.02–0.81 ppb in North America (Zhou et al., 2002a,b; Ren et al., 2010; Villena et al., 2011; N. Zhang et al., 2012; Wong et al., 2012; VanderBoer et al., 2013), 2.00 ppb (maximum) in South America (Elshorbany et al., 2009), and 0.015–0.02 ppb in Antarctica (Kerbrat et al., 2012) (Fig. 1).”

6) Lines 79-81 “These high HONO mixing ratios, particularly in the daytime, cannot be explained well by gas-phase production (Reaction R1), suggesting that an unknown daytime HONO source (P_{unknown}) could exist.” Here, the authors were clearly defining the P_{unknown} . The definition is contradictory to the part presented on lines 36-50.

The revision was made in the introduction section: “These high HONO mixing ratios, particularly in the daytime, cannot be explained well by gas-phase production [Reaction (R1)], HONO emissions, and nighttime hydrolysis conversion of NO_2 on aerosols, suggesting that an unknown daytime HONO source (P_{unknown}) could exist.”

7) If what presented on lines 91-118 are reasonable, the definition of P_{unknown} on lines 79-81 is problematic and authors should redefine P_{unknown} .”

The definition of P_{unknown} was clarified in the entire manuscript. The hydrolysis reaction of nitrogen dioxide (NO_2) on humid surfaces in this paper only happened in the nighttime.

8) Section 2.1, the authors should explain explicitly why the dataset was used for testing.

The description in Section 2.1 was added: “Anthropogenic emissions were based on the year 2006/2007. Limited measurements of HONO, OH, and HO₂ in the coastal regions of China were made in the summers of 2006/2007, so these limited measurements were used for model evaluation.”

9) Lines 192-194, the description is inconsistent with what the authors defined early. The sentences are suggesting what the authors’ analysis presented before is also problematic. They need to be rewording.

Please see our responses to questions 2, 6, and 7.

10) Lines 214-215, please define coastal regions of China.

The description of coastal regions of China was added in section 2.2: “For the coastal regions of China (mainly including Laoning, Beijing, Tianjin, Hebei, Shandong, Jiangsu, Anhui, Shanghai, Zhejiang, Jiangxi, Fujian, and Guangdong), ...”

11) Lines 253-273, the authors should explain the metrics rather than listing the numbers.

The description in Section 3.1 was added: “The statistical metrics of mean bias (MB), mean error (ME), root-mean-square error (RMSE), normalized mean bias (NMB), normalized mean error (NME), index of agreement (IOA), and correlation coefficient (CC), were used. The MB, ME, and RMSE are given in the same units as the measurements (absolute metrics). The MB quantifies the tendency of the model to over- or underestimate values, while the ME and RMSE measure the magnitude of the difference between modeled and observed values regardless of whether the modeled values are higher or lower than observations. One disadvantage of absolute metrics is that they make intercomparisons of model performance in clean and polluted environments or across different pollutants difficult to interpret.

Consequently, a range of relative metrics are often used. These metrics are presented either in fractional or percentage units. The NMB and NME all normalize by observed values. The IOA and CC provide a sense of the strength of the relationship between model estimates and observations that have been paired in time and space. Perfect agreement for any metric alone may not be indicative of good model performance, so multiple metrics must be considered when evaluating model performance.”

12) Lines 253-288, the part does not read well and needs language editing.

Minor revisions were made and shown in section 3.1.

13) Lines 289-295, try to use numbers instead of words such as minor, noticeable and substantial.

The description in Section 3.1 was revised: “Simulated diurnal variations of OH and HO₂ showed consistent patterns with the observed data (Fig. 6). When HONO emissions and Reaction (R4) were considered (case R_{wop}), OH and HO₂ enhancements were $\leq \sim 6\%$ in most cases compared with case R (Fig. 6 and Table 3), but the P_{unknown} led to 10%–150% improvements in OH simulations on 5–12 July 2006 (Fig. 6). The 20%–90% overestimation of OH mixing ratios on 20–25 July 2006 (Fig. 6) needs further investigation. Compared with case R, the NME was reduced by 79.60% (=136.60% – 57.00%), whereas the NMB was increased by 105.40% (123.00% – 17.60%), and the IOA was improved to 0.84 from 0.79 (Table 3).

14) Lines 295-296, how come so many effective numbers for NME and NMB? The same problems are also applicable for other parts.”

Please see our response to question 13.

15) Lines 304-312, the logic is not straightforward and need to reorganize.

The description in Section 3.2 was revised: “High $P_{unknown}$ values were found in the coastal regions of China (Fig. 7), especially in the BTH, YRD and PRD regions due to elevated emissions of NO_x (Zhang et al., 2009). The largest daytime average $P_{unknown}$ value reached 2.5 ppb h^{-1} in Tianjin of the BTH region (Fig. 7a), whereas it was 2.0 ppb h^{-1} in Shanghai of the YRD region (Fig. 7b). The largest daytime average $P_{unknown}$ value reached 1.2 ppb h^{-1} in Guangzhou and Shenzhen of the PRD (Fig. 7c), lower than the values of 2.5 ppb h^{-1} and 2.0 ppb h^{-1} . One major reason is the underestimation of daytime NO_2 mixing ratios in the PRD (Fig. 4b).”

16) Lines 351-358, why sometimes use the average, but sometimes use the maximum. The jump is very confusing.

The description in Section 3.3 was revised: “Incorporation of the $P_{unknown}$ into the WRF-Chem model led to substantial enhancements in the daytime average mixing ratios of OH in the coastal regions of China, e.g., 60%–190% in the BTH region, 60%–210% in the YRD region, and 60%–200% in the PRD region (Fig. 9a). The maximum enhancement of HO_2 reached 250% in the BTH region, 200% in the YRD region, and 140% in the PRD region (Fig. 9b). Similarly, a daytime average increase of 100%–180%, 60%–150% and 40%–80% in RO_2 [$= CH_3O_2$ (methylperoxy radical) + $ETHP$ (ethylperoxy radical) + C_2O_3 (peroxyacyl radical) + others] were found in the BTH, YRD and PRD regions, respectively (Fig. 9c).”

17) Lines 362-365, the sentences are not readable and need to be written.

The description in Section 3.3 was revised: “Vertically, the $P_{unknown}$ enhanced the monthly meridional-mean daytime (06:00–18:00 LST) mixing ratios of OH, HO_2 and RO_2 by 5%–38%, 5%–47% and 5%–48%, respectively, within 1000 m above the ground in the coastal regions of China (Fig. 10). Strong vertical mixing in the daytime in summer led to a roughly uniform vertical enhancement of OH, HO_2 and RO_2 within the 1000 m at the same latitude (Fig. 10). Different $P_{unknown}$ values in different latitudes produced distinct differences in the enhancements of OH, HO_2 and RO_2 , with a maximum located near 35°N (Fig. 10).”

18) Section 3.3 is short, but Section 3.4 is so long and need to be cut. The current form of Section 3.4 is difficult to follow.

The description in Section 3.4 was shortened: *“OH radicals are produced mainly through the reaction of $\text{HO}_2 + \text{NO}$, the photolysis of O_3 and HONO, and the reactions between O_3 and alkenes (Fig. 11). For case R, the predominant contribution to $P(\text{OH})$ (production rate of OH) was the reaction of $\text{HO}_2 + \text{NO}$ (Fig. S1a, c, e), and the photolysis of O_3 was the second most important source of OH (Fig. S1a, c, e). When the three additional HONO sources were added, the most important source was the reaction of $\text{HO}_2 + \text{NO}$, with a diurnal maximum conversion rate reaching 9.38 [7.23 due to the P_{unknown}] ppb h^{-1} in Beijing, 2.63 [1.15] ppb h^{-1} in Shanghai, and 4.88 [1.43] ppb h^{-1} in Guangzhou near noon (Fig. 11a, c, e). The photolysis of HONO became the second most important source of OH in Beijing and Guangzhou before 10:00 LST, and in Shanghai before 12:00 LST; the diurnal peaks were 3.72 [3.06] ppb h^{-1} in Beijing at 09:00 LST, 0.89 [0.62] ppb h^{-1} in Shanghai at 11:00 LST, and 0.97 [0.78] ppb h^{-1} in Guangzhou at 09:00 LST (Fig. 11a, c, e), which were comparable to or lower than the 3.10 ppb h^{-1} reported by Elshorbany et al. (2009). Kanaya et al. (2009), who also conducted similar studies at Mount Tai (located in a rural area) of China, using an observationally constrained box model, suggested that the reaction of $\text{HO}_2 + \text{NO}$ was the predominant OH source, with a daytime average of 3.72 ppb h^{-1} , more than the 1.38 ppb h^{-1} of the photolysis of O_3 . Using an observationally constrained box model, Hens et al. (2014) reported similar results in a boreal forest, in which the dominant contributor to OH was the reaction of $\text{HO}_2 + \text{NO}$, ranging from 0.23 to 1.02 ppb h^{-1} during daytime. The production rates of OH in our study were higher than in Kanaya et al. (2009) and Hens et al. (2014) due to higher NO_x emissions in urban areas than in rural areas.*

The dominant loss rate of OH was the reaction of $\text{OH} + \text{NO}_2$ for both cases R and R_p (Figs. 11b, d, f and S1b, d, f). The diurnal maximum loss rates were 1.98 ppb h^{-1} in Beijing, 1.12 ppb h^{-1} in Shanghai, and 1.70 ppb h^{-1} in Guangzhou for case R (Fig. S1b, d, f), whereas these values were 5.61 [4.38 due to the P_{unknown}] ppb h^{-1} in

Beijing, 2.00 [1.00] ppb h⁻¹ in Shanghai, and 2.65 [1.02] ppb h⁻¹ in Guangzhou for case R_p (Fig. 11b, d, f). The reactions of OH + VOCs to form HO₂ and RO₂ were the second most important loss path of OH, with a diurnal maximum of 0.75–1.73 ppb h⁻¹ for case R (Fig. S1b, d, f) and 1.57 [0.82 due to the P_{unknown}] to 5.37 [4.05] ppb h⁻¹ for case R_p in Beijing, Shanghai and Guangzhou (Fig. 11b, d, f). The third most important OH loss path was the reaction of OH + CO to form HO₂; the diurnal maximum rates were 0.46–1.47 ppb h⁻¹ for case R (Fig. S1b, d, f) and 0.93 [0.49 due to the P_{unknown}] to 3.58 [2.86] ppb h⁻¹ for case R_p in Beijing, Shanghai and Guangzhou (Fig. 11b, d, f).

The averaged radical conversion rates in the daytime (06:00–18:00 LST) are illustrated in Fig. 12. OH radicals are produced mainly via the photolysis of O₃, HONO and hydrogen peroxide (H₂O₂), and the reactions between O₃ and alkenes, after which OH radicals enter the RO_x (= OH + HO₂ + RO₂) cycle (Fig. 12 and Tables 4, S2 and S3). For case R, the reaction of HO₂ + NO was the major source of OH [2.78 ppb h⁻¹ (81.73% of the total daytime average production rate of OH) in Beijing, 0.73 ppb h⁻¹ (67.09%) in Shanghai, and 1.75 ppb h⁻¹ (71.54%) in Guangzhou] (Fig. 12a and Table 4). The second largest source of OH was the photolysis of O₃ (Table 4). OH radicals were removed mainly through the reaction of OH + NO₂ [1.12 ppb h⁻¹ (39.31% of the total daytime average loss rate of OH) in Beijing, 0.47 ppb h⁻¹ (46.63%) in Shanghai, and 0.77 ppb h⁻¹ (38.33%) in Guangzhou] (Table 4), whereas those were converted to HO₂ mainly via the reaction of OH + CO (Table 4). For HO₂, the predominant production pathways were the reactions of OH + CO and CH₃O₂ + NO and the photolysis of formaldehyde (HCHO) (Table S2). HO₂ radicals were consumed primarily via the reaction of HO₂ + NO [2.78 ppb h⁻¹ (99.34%) in Beijing, 0.73 ppb h⁻¹ (99.61%) in Shanghai, and 1.75 ppb h⁻¹ (98.29%) in Guangzhou] (Table S2). RO₂ radicals were formed mainly from the reactions of OH + OLET (terminal olefin carbons)/OLEI (internal olefin carbons), OH + ETH (ethene), OH + methane (CH₄), and OH + AONE (acetone). RO₂ radicals were consumed primarily via the reaction of CH₃O₂ + NO [0.54 ppb h⁻¹ (94.56%) in Beijing, 0.16 ppb h⁻¹ (95.28%) in Shanghai, and 0.33 ppb h⁻¹ (96.07%)

in Guangzhou] (Table S3).

When the three additional HONO sources were inserted into the WRF-Chem model (case R_p), the daytime average OH production rate was enhanced by 4.32 (= 7.10 – 2.78) [3.86 due to the $P_{unknown}$] ppb h^{-1} in Beijing, 0.67 (= 1.40 – 0.73) [0.64] ppb h^{-1} in Shanghai, and 0.80 (= 2.55 – 1.75) [0.68] ppb h^{-1} in Guangzhou via the reaction of $\text{HO}_2 + \text{NO}$, and by 1.86 [1.86] ppb h^{-1} in Beijing, 0.50 [0.50] ppb h^{-1} in Shanghai, and 0.49 [0.47] ppb h^{-1} in Guangzhou via the photolysis of HONO, respectively (Table 4). The enhancements of the daytime average OH production rate due to the photolysis of HONO were comparable to or lower than the 2.20 ppb h^{-1} obtained by Liu et al. (2012). The daytime average OH loss rate was increased by 2.03 [1.92 due to the $P_{unknown}$] ppb h^{-1} in Beijing, 0.58 [0.55] ppb h^{-1} in Shanghai, and 0.65 [0.58] ppb h^{-1} in Guangzhou via the reaction of $\text{OH} + \text{NO}_2$, and by 1.78 [1.64] ppb h^{-1} in Beijing, 0.31 [0.28] ppb h^{-1} in Shanghai, and 0.42 [0.36] ppb h^{-1} in Guangzhou via the reaction of $\text{OH} + \text{CO}$, respectively (Table 4). Similarly, the daytime average HO_2 production rate was increased by 0.31 [0.28 due to the $P_{unknown}$] to 1.78 [1.64] ppb h^{-1} in Beijing, Shanghai and Guangzhou via the reaction of $\text{OH} + \text{CO}$, and by 0.63 [0.59] ppb h^{-1} in Beijing, 0.10 [0.09] ppb h^{-1} in Shanghai, and 0.19 [0.17] ppb h^{-1} in Guangzhou via the reaction of $\text{CH}_3\text{O}_2 + \text{NO}$; whereas, the daytime average HO_2 loss rate was enhanced by 0.67 [0.61 due to the $P_{unknown}$] to 4.32 [4.27] ppb h^{-1} in Beijing, Shanghai and Guangzhou via the reaction of $\text{HO}_2 + \text{NO}$ (Table S2).

Overall, the net daytime production rate of RO_x was increased to 3.48 (= 2.56 + 0.71 + 0.21) [2.06 due to the $P_{unknown}$] from 1.20 (= 0.60 + 0.43 + 0.17) ppb h^{-1} in Beijing, 1.09 (= 0.86 + 0.19 + 0.04) [0.45] from 0.54 (= 0.36 + 0.14 + 0.04) ppb h^{-1} in Shanghai, and 1.52 (= 1.21 + 0.26 + 0.05) [0.58] from 0.92 (= 0.68 + 0.20 + 0.04) ppb h^{-1} in Guangzhou (Fig. 12) due to the three additional HONO sources, indicating that the RO_x source was mainly from OH production, especially via the photolysis of HONO (Tables 4, S2 and S3). This result is different from the conclusion of Liu et al. (2012) that the photolysis of HONO and oxygenated VOCs is the largest RO_x source. One of the primary reasons for this is the underestimation of

anthropogenic VOCs (Wang et al., 2014). For Beijing, the net production rate of RO_x was 3.48 ppb h^{-1} , lower than the 6.60 ppb h^{-1} from the field studies of Liu et al. (2012). Our results reconfirmed the view of Ma et al. (2012) that the North China Plain acts as an oxidation pool. The additional HONO sources produced an increase in the net loss rate of RO_x from 1.25 to 3.28 [1.96 due to the P_{unknown}] ppb h^{-1} in Beijing, 0.53 to 1.09 [0.54] ppb h^{-1} in Shanghai, and 0.85 to 1.51 [0.59] ppb h^{-1} in Guangzhou (Fig. 12)."

19) The authors need to justify why BTH, YRD and PRD are selected for discussing, but not other cities.

The revisions were made and shown in section 2.3 of the revised version: *"Two domains with a horizontal resolution of 27 km were employed in this study: domain 1 covered East Asia, whereas domain 2 covered the coastal regions of China, including the Beijing–Tianjin–Hebei region (BTH), the Yangtze River delta (YRD), and the Pearl River delta (PRD) (Fig. 3), which are the three most rapidly-developing economic growth regions of China. The rapid economic development and urbanization has led to a serious deterioration in air quality in these three regions. Beijing, Shanghai, and Guangzhou are three representative cities of the three regions, so this study focuses on the three regions, including the three representative cities."*

20) Lines 367-376 can be cut largely because the similar results should be well documented in literature.

Accepted. Thanks. The revisions were shown in section 3.4.

21) Lines 385-294, does Kanaya et al. (2009) and Hens et al. (2014) use the same approach for P_{unknown} ? This should be clarified.

The description in Section 3.4 was revised: *"Kanaya et al. (2009), who also conducted similar studies at Mount Tai (located in a rural area) of China, using an observationally constrained box model, suggested that the reaction of $HO_2 + NO$ was the predominant OH source, with a daytime average of 3.72 ppb h^{-1} , more than*

the 1.38 ppb h^{-1} of the photolysis of O_3 . Using an observationally constrained box model, Hens et al. (2014) reported similar results in a boreal forest, in which the dominant contributor to OH was the reaction of $\text{HO}_2 + \text{NO}$, ranging from 0.23 to 1.02 ppb h^{-1} during daytime. The production rates of OH in our study were higher than in Kanaya et al. (2009) and Hens et al. (2014) due to higher NO_x emissions in urban areas than in rural areas.

22) Lines 408-416 can also be cut largely since similar results should be well documented in literature.

Accepted. Thanks. The revisions were shown in section 3.4.

23) Lines 417-487, the authors listed so many numbers which have been shown either in Tables and Figures. The authors should try to summarize these results to make the analysis to be easily understood.

The description in Section 3.4 was revised.

24) Conclusion can be largely cut since they duplicate.

The description in the conclusion section was largely cut: “The relationship between the P_{unknown} , NO_2 mixing ratios and $J(\text{NO}_2)$ was investigated using available data from 13 field studies across the globe. The formula $P_{\text{unknown}} \approx 19.60[\text{NO}_2] \cdot J(\text{NO}_2)$ was obtained, and then the three additional HONO sources (i.e., the P_{unknown} , HONO emissions and nighttime hydrolysis conversion of NO_2 on aerosols) were inserted into the WRF-Chem model, to assess the P_{unknown} impacts on the concentrations and budgets of HONO and RO_x in the coastal regions of China. The results showed that:

(1) The additional HONO sources led to significant improvements in the simulations of HONO and OH, especially in the daytime.

(2) Elevated daytime average P_{unknown} values were found in the coastal regions of China, reaching 2.5 ppb h^{-1} in the BTH region, 2.0 ppb h^{-1} in the YRD region, and 1.2 ppb h^{-1} in the PRD region.

(3) The additional HONO sources substantially enhanced the production and

loss rates of HONO. Dry deposition of HONO contributed 0.28–0.45 ppb h⁻¹ to the loss rate of HONO, approximately equivalent to the contribution of HONO emissions, emphasizing the importance of dry deposition of HONO in high NO_x emissions areas.

(4) The P_{unknown} produced a 60%–210% enhancement of OH, a 60%–250% enhancement of HO₂, and a 60%–180% enhancement of RO₂ near the ground in the major cities of the coastal regions of China. Vertically, the P_{unknown} enhanced the daytime meridional-mean mixing ratios of OH, HO₂ and RO₂ by 5%–38%, 5%–47% and 5%–48%, respectively, within 1000 m above the ground.

(5) When the three additional HONO sources were added, the photolysis of HONO became the second most important source of OH in Beijing and Guangzhou before 10:00 LST, and in Shanghai before 12:00 LST, with a maximum of 3.72 [3.06 due to the P_{unknown}] ppb h⁻¹ in Beijing, 0.89 [0.62] ppb h⁻¹ in Shanghai, and 0.97 [0.78] ppb h⁻¹ in Guangzhou; whereas, the reaction of HO₂ + NO was the most important source of OH, dominated in Beijing and Guangzhou after 10:00 LST and in Shanghai after 12:00 LST, with a maximum of 9.38 [7.23] ppb h⁻¹ in Beijing, 2.63 [1.15] ppb h⁻¹ in Shanghai, and 4.88 [1.43] ppb h⁻¹ in Guangzhou.

Overall, the above results suggest that the P_{unknown} significantly enhances the atmospheric oxidation capacity in the coastal regions of China by increasing RO_x concentrations and accelerating RO_x cycles, and could lead to considerable increases in concentrations of inorganic aerosols and secondary organic aerosols and further aggravate haze events in these regions.”

2. The list of all relevant changes made in the revised manuscript below

A. Change for “Title”

- 1) Lines 1-3

B. Changes for “Abstract”

- 1) Lines 15-16
- 2) Lines 19-20
- 3) Line 26
- 4) Lines 31-37
- 5) Lines 44-45

C. Changes for “1. Introduction”

- 1) Lines 73-81
- 2) Lines 82-84

D. Changes for “2.1 Observed data”

- 1) Lines 179-182
- 2) Lines 184-185
- 3) Lines 188-189

E. Changes for “2.2 Parameterization of HONO sources”

- 1) Lines 219-223

F. Changes for “2.3 Model setup”

- 1) Lines 238-243

G. Changes for “3.1 Comparison of simulations and observations”

- 1) Lines 262-277
- 2) Line 296
- 3) Lines 313-318

H. Changes for “3.2 P_{unknown} simulations and its impacts on production and loss rates of HONO”

1) Lines 328-332

2) Lines 366-369

I. Changes for “3.3 P_{unknown} impacts on concentrations of OH, HO₂ and RO₂”

1) Lines 376-377

2) Lines 383-387

J. Changes for “3.4 P_{unknown} impacts on the budgets of OH, HO₂ and RO₂”

1) Lines 390-393

2) Lines 403-404

3) Line 406

4) Lines 423-427

5) Lines 431-437

6) Lines 442-444

7) Lines 445-464

8) Line 465

9) Line 469

10) Lines 477-479

K. Changes for “4. Conclusions”

1) Line 483

2) Lines 493-509

3. The marked-up manuscript version (Changes are in red font)

Impacts of an unknown daytime HONO source on the mixing ratio and budget of HONO, and hydroxyl, hydroperoxyl and organic peroxy radicals, in the coastal regions of China

Yujia Tang^{1,2}, Junling An^{1*}, Feng Wang^{1,2,3}, Ying Li¹, Yu Qu¹, Yong Chen¹, Jian Lin^{1,2}

¹State Key Laboratory of Atmospheric Boundary Layer Physics and Atmospheric Chemistry (LAPC), Institute of Atmospheric Physics (IAP), Chinese Academy of Sciences, Beijing 100029, China

²University of the Chinese Academy of Sciences, Beijing 100049, China

³Anhui Meteorological Bureau, Hefei 230061, China

*Corresponding author: anjl@mail.iap.ac.cn

Abstract

Many field experiments have found high nitrous acid (HONO) mixing ratios in both urban and rural areas during daytime, but these high daytime HONO mixing ratios cannot be explained well by gas-phase production, HONO emissions, and nighttime hydrolysis conversion of nitrogen dioxide (NO₂) on aerosols, suggesting that an unknown daytime HONO source (P_{unknown}) could exist. The formula $P_{\text{unknown}} \approx 19.60[\text{NO}_2] \cdot J(\text{NO}_2)$ was obtained using observed data from 13 field experiments across the globe. The three additional HONO sources (i.e., the P_{unknown} , nighttime hydrolysis conversion of NO₂ on aerosols, and HONO emissions) were coupled into the WRF-Chem model (Weather Research and Forecasting model coupled with Chemistry) to assess the P_{unknown} impacts on the concentrations and budgets of HONO and peroxy (hydroxyl, hydroperoxyl, and organic peroxy) radicals (RO_x) (= OH + HO₂ + RO₂) in the coastal regions of China. Results indicated that the additional HONO sources produced a significant improvement in HONO and OH simulations, particularly in the daytime. High daytime average P_{unknown} values were

found in the coastal regions of China, with a maximum of 2.5 ppb h^{-1} in the Beijing–Tianjin–Hebei region. The P_{unknown} produced a 60%–250% increase of OH, HO_2 and RO_2 near the ground in the major cities of the coastal regions of China, and a 5%–48% increase of OH, HO_2 and RO_2 in the daytime meridional-mean mixing ratios within 1000 m above the ground. When the three additional HONO sources were included, the photolysis of HONO was the second most important source in the OH production rate in Beijing, Shanghai and Guangzhou before 10:00 LST with a maximum of 3.72 ppb h^{-1} and a corresponding P_{unknown} contribution of 3.06 ppb h^{-1} in Beijing, whereas the reaction of $\text{HO}_2 + \text{NO}$ (nitric oxide) was dominant after 10:00 LST with a maximum of 9.38 ppb h^{-1} and a corresponding P_{unknown} contribution of 7.23 ppb h^{-1} in Beijing. The whole RO_x cycle was accelerated by the three additional HONO sources, especially the P_{unknown} . The daytime average OH production rate was enhanced by 0.67 due to the three additional HONO sources [0.64 due to the P_{unknown}] to $4.32 [3.86] \text{ ppb h}^{-1}$ via the reaction of $\text{HO}_2 + \text{NO}$, and by 0.49 [0.47] to $1.86 [1.86] \text{ ppb h}^{-1}$ via the photolysis of HONO, and the OH daytime average loss rate was enhanced by 0.58 [0.55] to $2.03 [1.92] \text{ ppb h}^{-1}$ via the reaction of $\text{OH} + \text{NO}_2$ and by 0.31 [0.28] to $1.78 [1.64] \text{ ppb h}^{-1}$ via the reaction of $\text{OH} + \text{CO}$ (carbon monoxide) in Beijing, Shanghai and Guangzhou. Similarly, the three additional HONO sources produced an increase of 0.31 [corresponding P_{unknown} contribution of 0.28] to $1.78 [1.64] \text{ ppb h}^{-1}$ via the reaction of $\text{OH} + \text{CO}$ and 0.10 [0.09] to $0.63 [0.59] \text{ ppb h}^{-1}$ via the reaction of CH_3O_2 [methylperoxy radical] + NO in the daytime average HO_2 production rate, and 0.67 [0.61] to $4.32 [4.27] \text{ ppb h}^{-1}$ via the reaction of $\text{HO}_2 + \text{NO}$ in the daytime average HO_2 loss rate in Beijing, Shanghai and Guangzhou. The above results suggest that the P_{unknown} considerably enhanced the RO_x concentrations and accelerated RO_x cycles in the coastal regions of China, and could produce significant

increases in concentrations of inorganic aerosols and secondary organic aerosols and further aggravate haze events in these regions.

1. Introduction

The hydroxyl radical (OH) is the dominant oxidant in the troposphere, initiating daytime photochemistry, removing the majority of reactive gases, and leading to the formation of secondary products [e.g. ozone (O_3), PANs (peroxyacyl nitrates) and aerosols] that can affect air quality, climate, and human health (Stone et al., 2012). OH is formed primarily through the photolysis of O_3 , nitrous acid (HONO), hydrogen peroxide (H_2O_2), the reactions of O_3 with alkenes, and the hydroperoxyl radical (HO_2) to OH conversion process (HO_2+NO) (Platt et al., 1980; Crutzen and Zimmermann, 1991; Atkinson and Aschmann, 1993; Fried et al., 1997; Paulson et al., 1997). Recent field experiments have found that the contribution of the photolysis of HONO to daytime OH production can reach up to 56%, 42% and 33% in urban, rural and forest areas, respectively (Ren et al., 2003; Kleffmann et al., 2005; Acker et al., 2006), more than that of the photolysis of O_3 . However, most current air quality models fail to predict observed HONO concentrations, underestimating daytime HONO in particular (Czader et al., 2012; Gonçalves et al., 2012; Li et al., 2011), due to the incomplete knowledge of HONO sources.

It is generally accepted that the photolysis of HONO [Reaction (R2)] in the early morning could be a major source of OH. After sunrise, HONO mixing ratios are usually in low concentrations due to the strong photolysis of HONO. However, many field experiments have found daytime HONO mixing ratios that are unexpectedly higher than the theoretical steady value (~10 ppt), in both urban and rural areas: e.g., 0.15–1.50 ppb in Asia (Su et al., 2008; Wu et al., 2013; Spataro et al., 2013),

0.01–0.43 ppb in Europe (Kleffmann et al., 2005; Acker et al., 2007; Sörgel et al., 2011; Michoud et al., 2014), 0.02–0.81 ppb in North America (Zhou et al., 2002a,b; Ren et al., 2010; Villena et al., 2011; N. Zhang et al., 2012; Wong et al., 2012; VanderBoer et al., 2013), 2.00 ppb (maximum) in South America (Elshorbany et al., 2009), and 0.015–0.02 ppb in Antarctica (Kerbrat et al., 2012) (Fig. 1). These high HONO mixing ratios, particularly in the daytime, cannot be explained well by gas-phase production [Reaction (R1)], HONO emissions, and nighttime hydrolysis conversion of NO₂ on aerosols, suggesting that an unknown daytime HONO source (P_{unknown}) could exist.



The P_{unknown} was calculated by Su et al. (2008) at Xinken (Guangzhou, China), with a maximum of 4.90 ppb h⁻¹. Spataro et al. (2013) proposed a P_{unknown} value of 2.58 ppb h⁻¹ in Beijing. In fact, P_{unknown} values, ranging from 0.06 to 4.90 ppb h⁻¹ have been obtained from many field studies across the globe, as shown in Fig. 1, suggesting P_{unknown} could contribute greatly to the daytime production of OH and HO₂.

The most important formation pathway for nocturnal HONO could be the hydrolysis reaction of nitrogen dioxide (NO₂) on humid surfaces [Reaction (R4)] (Kleffmann et al., 1999; Alicke et al., 2002; Finlayson-Pitts et al., 2003):



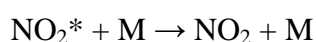
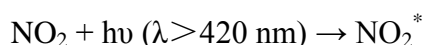
Ammann et al. (1998) found HONO formation via the heterogeneous reduction of NO₂ on the surface of soot [Reaction (R5)], and Reaction (R5) can be enhanced by irradiation (Monge et al., 2010):



George et al. (2005) and Stemmler et al. (2006, 2007) showed the heterogeneous reduction of NO₂ on organic surfaces [Reaction (R6)] (e.g. humic acid) to produce HONO:



Li et al. (2008) proposed a homogeneous reaction of photolytically excited NO₂ with H₂O [Reaction (R7)], but this reaction has been proven to be unimportant in the real atmosphere (Carr et al., 2009; Wong et al., 2011; Amedro et al., 2011). Zhang and Tao (2010) suggested the homogeneous nucleation of NO₂, H₂O and ammonia (NH₃) for the production of HONO [Reaction (R8)], but Reaction (R8) has not yet been tested in laboratory studies, nor observed in field experiments:



Zhou et al. (2002b, 2003, 2011) demonstrated that the photolysis of adsorbed nitric acid (HNO₃) and nitrate (NO₃⁻) at ultraviolet wavelengths (~300 nm) [Reaction (R9)] can produce HONO:



Additionally, HONO could be emitted from soils (Su et al., 2011; Oswald et al., 2013), and may be important in farmland and forest areas.

Based on these mechanisms outlined above, some modeling studies have been carried out to simulate HONO concentrations (e.g. An et al., 2011; Czader et al., 2012; Gonçalves et al., 2012). Sarwar et al. (2008) incorporated Reactions (R4), (R9) and HONO emissions into the Community Multiscale Air Quality (CMAQ) model, but still underestimated HONO mixing ratios during daytime. Li et al. (2010) considered

both aerosol and ground surface reactions, and HONO emissions, in the WRF-Chem model (Weather Research and Forecasting model coupled with Chemistry), and found that HONO simulations were significantly improved. However, Li et al. (2010) used a relatively high emissions ratio of 2.3% for HONO/NO₂ to compute the direct emissions of HONO, which could have overestimated the HONO concentrations in the air (An et al., 2013). Czader et al. (2012) added Reactions (R6), (R7) and HONO emissions into the CMAQ model. The HONO simulations matched well with observations at night, but were significantly lower than observations at noon. Wong et al. (2013) reported good agreement between simulated and observed daytime HONO when HONO emissions, photolytically enhanced daytime formation mechanisms on both aerosols and the ground, and Reaction (R7), were included. However, according to our recent studies (Tang et al., 2014), this result depended heavily on the selection of uptake coefficients of NO₂ heterogeneous chemistry. Overall, the topic of HONO sources remains under discussion today, and so it is a challenge for modelers to decide which mechanism(s) to be coupled into an air quality model.

To investigate the importance of the mechanisms described above, correlation tests between the P_{unknown} and NO₂, HNO₃, irradiation or the photolysis frequency of NO₂ [$J(\text{NO}_2)$] were conducted in field experiments (Acker et al., 2007; Sörgel et al., 2011; Villena et al., 2011; Wong et al., 2012). Many of these studies demonstrated that there is a clear dependency of the P_{unknown} on irradiation/ $J(\text{NO}_2)$ during daytime, particularly at noon. Rohrer et al. (2005) proposed that the photolytic HONO source at the surface of the chamber strongly depended on light intensity. Acker et al. (2007) summarized field experiments in several European countries and showed a strong correlation ($R^2=0.81$) between the P_{unknown} and $J(\text{NO}_2)$. Wong et al. (2012) also indicated that the P_{unknown} showed a clear symmetrical diurnal variation with a

maximum around noontime, closely correlated with actinic flux (NO_2 photolysis frequency) and solar irradiance; the correlation coefficient was over 0.70.

Besides irradiation/ $J(\text{NO}_2)$, good correlations between the P_{unknown} and NO_2 mixing ratios have been found from both field and laboratory studies, supporting the viewpoint that NO_2 is the primary precursor of HONO. Through estimating the P_{unknown} , Acker et al. (2007) speculated that the daytime HONO levels might be explained by a fast electron transfer onto adsorbed NO_2 . Sörgel et al. (2011) indicated that the conversion of NO_2 most likely accounted for light-induced HONO formation, about an order of magnitude stronger than HONO formation during nighttime. High correlations between the P_{unknown} and NO_2 mixing ratios have also been found [e.g., $R^2 = 0.77$ in Qin et al. (2006), $R^2 = 0.80$ in Villena et al. (2011), and $R^2 = 0.62$ in Elshorbany et al. (2009)], indicating that the photosensitized conversion of NO_2 is more likely to be the daytime HONO source. This is the reason why the recent CalNex 2010 (California Research at the Nexus of Air Quality and Climate Change) study found a very strong positive correlation ($R^2 = 0.985$) between HONO flux and the product of NO_2 concentration and solar radiation at the Bakersfield site (Ren et al., 2011).

Based on the studies introduced above, the P_{unknown} calculated from field experiments may be a practical method to help quantify the daytime HONO source. In this study, field experiment data from 13 different field campaigns across the globe were used to express the P_{unknown} as a function of NO_2 mixing ratios and $J(\text{NO}_2)$ (see Sect. 2.2). We then added the P_{unknown} into the WRF-Chem model to assess the impacts of the P_{unknown} on the concentrations and production and loss rates of HONO, OH, HO_2 , and organic peroxy radicals (RO_2).

2. Data and methods

2.1 Observed data

Anthropogenic emissions were based on the year 2006/2007. Limited measurements of HONO, OH, and HO₂ in the coastal regions of China were made in the summers of 2006/2007, so these limited measurements were used for model evaluation. Observed air temperature (TA), relative humidity (RH), wind speed (WS) and direction (WD) near the ground were obtained from the National Climatic Data Center, China Meteorological Administration (H. Zhang et al., 2012). Surface mixing ratios of O₃ and NO₂ in Beijing were obtained from the Beijing Atmospheric Environmental Monitoring Action, carried out by the Chinese Academy of Sciences (Li et al., 2011; Wang et al., 2014), except those in Guangzhou, which were sourced from Qin et al. (2009). HONO observations were conducted using two annular denuders at the campus of Peking University (39°59'N, 116°18'E) in Beijing on 17–20 August 2007 (Spataro et al., 2013) and a long path absorption photometer at the Backgarden (BG) supersite (23°30'N, 113°10'E), about 60 km northwest of Guangzhou on 3–31 July 2006 (X. Li et al., 2012). The measurement systems are described in detail in Spataro et al. (2013) and X. Li et al. (2012). OH and HO₂ were measured by laser induced fluorescence at the BG supersite on 3–30 July 2006 (Lu et al., 2012).

2.2 Parameterization of HONO sources

Besides HONO gas-phase production from Reaction (R1), three additional HONO sources [HONO emissions, Reaction (R4) (nighttime), and the P_{unknown}] were coupled into the WRF-Chem model in this work.

HONO emissions were calculated using $[0.023 \times f_{\text{DV}} + 0.008 \times (1 - f_{\text{DV}})] \times f_{\text{TS}}$,

where f_{DV} denotes the nitrogen oxides (NO_x) emissions ratio of diesel vehicles to total vehicles, and f_{TS} is the NO_x emissions ratio of the traffic source to all anthropogenic sources (Li et al., 2011; An et al., 2013; Tang et al., 2014). Reaction (R4) was inserted into the Carbon-Bond Mechanism Z (CBM-Z) during nighttime only. The heterogeneous reaction rate was parameterized by $k = \left(\frac{a}{D_g} + \frac{4}{v\gamma} \right)^{-1} A_s$ (Jacob, 2000), where a is the radius of aerosols, v is the mean molecular speed of NO_2 , D_g is a gas-phase molecular diffusion coefficient taken as $10^{-5} \text{ m}^2 \text{ s}^{-1}$ (Dentener and Crutzen, 1993), and A_s is the aerosol surface area per unit volume of air, calculated from aerosol mass concentrations and number density in each bin set by the Model for Simulating Aerosol Interactions and Chemistry (MOSAIC). Hygroscopic growth of aerosols was considered (Li et al., 2011).

Previous studies (Sörgel et al., 2010; Villena et al., 2011; Wong et al., 2012) have shown $P_{\text{unknown}} \propto [\text{NO}_2] \cdot J(\text{NO}_2)$. To quantify the relationship between the P_{unknown} and NO_2 mixing ratios and irradiation, daytime P_{unknown} , NO_2 mixing ratios and $J(\text{NO}_2)$, based on all the available data sets from 13 different field campaigns across the globe (Table S1), were plotted in Fig. 2. As expected, good correlation ($R^2 = 0.75$) between the P_{unknown} and NO_2 mixing ratios was obtained (Fig. 2a). Furthermore, the correlation between the P_{unknown} and $[\text{NO}_2] \cdot J(\text{NO}_2)$ was increased to 0.80, with a linear regression slope of 19.60 (Fig. 2b). For the coastal regions of China (mainly including Laoning, Beijing, Tianjin, Hebei, Shandong, Jiangsu, Anhui, Shanghai, Zhejiang, Jiangxi, Fujian, and Guangdong), the correlation between the P_{unknown} and $[\text{NO}_2] \cdot J(\text{NO}_2)$ was 0.48, with a linear regression slope of 17.37 (Fig. S2b), which is within the maximum P_{unknown} uncertainty range of 25% (Table S1). The P_{unknown} cloud be expressed as a function of NO_2 mixing ratios and $J(\text{NO}_2)$, i.e.,

$P_{\text{unknown}} \approx 19.60[\text{NO}_2] \cdot J(\text{NO}_2)$. This formula is very similar to
 $P_{\text{unknown}} \approx \alpha \cdot J(\text{NO}_2) \cdot [\text{NO}_2] \cdot [\text{H}_2\text{O}] \cdot (S/V_g + S/V_a)$ proposed by Su et al. (2008), and
 $P_{\text{unknown}} \approx 3.3 \times 10^{-8}[\text{NO}_2] \cdot Q_s$ suggested by Wong et al. (2012) as an additional
daytime source of HONO through analysis of observed data, where S/V_a is the
aerosol surface area-to-volume ratio, S/V_g is the ground surface area-to-volume ratio,
 α is a fitting parameter, and Q_s is solar visible irradiance.

2.3 Model setup

Used in this study was the WRF-Chem model version 3.2.1 (Grell et al., 2005;
Fast et al., 2006), with the CBM-Z (Zaveri and Peters, 1999) and the MOSAIC
(Zaveri et al., 2008). The detailed physical and chemical schemes for the simulations
can be found in Tang et al. (2014). Two domains with a horizontal resolution of 27 km
were employed in this study: domain 1 covered East Asia, whereas domain 2 covered
the coastal regions of China, including the Beijing–Tianjin–Hebei region (BTH), the
Yangtze River delta (YRD), and the Pearl River delta (PRD) (Fig. 3), **which are the**
three most rapidly-developing economic growth regions of China. The rapid
economic development and urbanization has led to a serious deterioration in air
quality in these three regions. Beijing, Shanghai, and Guangzhou are three
representative cities of the three regions, so this study focuses on the three regions,
including the three representative cities. There were 28 vertical model layers from the
ground to 50 hPa, and the first model layer was ~28 m above the ground.
Meteorological initial and boundary conditions were obtained from the NCEP
(National Centers for Environmental Prediction) 1°×1° reanalysis dataset. Chemical
initial and boundary conditions were constrained with the output of MOZART-4
(Model for Ozone and Related chemical Tracers, version 4) (Emmons et al., 2010),

every 6 h. Monthly anthropogenic emissions in 2006/2007 and biogenic emissions were the same as those used by Li et al. (2011) and An et al. (2013).

Six simulations (cases R, R_{wop}, and R_p, performed for the entire months of August 2007 and July 2006), with a spin-up period of seven days, were conducted to assess the P_{unknown} effects on the concentrations and budgets of HONO, OH, HO₂, and RO₂. Case R only considered Reaction (R1) as a reference; Case R_{wop} included case R with HONO emissions, and Reaction (R4) only at night; case R_p contained case R_{wop} with the P_{unknown} [$\approx 19.60[\text{NO}_2] \cdot \text{J}(\text{NO}_2)$]. The P_{unknown} and Reaction (R4) were added to the CBM-Z, and diagnostic variables (i.e., production and loss rates of HONO, OH, HO₂, RO₂, O₃, and other species) were inserted into the CBM-Z to quantify the P_{unknown} impacts on the budgets of HONO, OH, HO₂, and RO₂ (Wang et al., 2014).

3. Results and discussion

3.1 Comparison of simulations and observations

The statistical metrics of mean bias (MB), mean error (ME), root-mean-square error (RMSE), normalized mean bias (NMB), normalized mean error (NME), index of agreement (IOA), and correlation coefficient (CC), were used. The MB, ME, and RMSE are given in the same units as the measurements (absolute metrics). The MB quantifies the tendency of the model to over- or underestimate values, while the ME and RMSE measure the magnitude of the difference between modeled and observed values regardless of whether the modeled values are higher or lower than observations. One disadvantage of absolute metrics is that they make intercomparisons of model performance in clean and polluted environments or across different pollutants difficult to interpret. Consequently, a range of relative metrics are often used. These metrics are presented either in fractional or percentage units. The NMB and NME all normalize by observed values. The IOA and CC provide a sense of the strength of the

relationship between model estimates and observations that have been paired in time and space. Perfect agreement for any metric alone may not be indicative of good model performance, so multiple metrics must be considered when evaluating model performance. Simulations of TA, RH, WS and WD were compared with observations, as shown in Wang et al. (2014). The MB, ME, RMSE, NMB, NME, IOA, and CC were comparable with those of Wang et al. (2010) and L. Li et al. (2012) using MM5 (the fifth-generation Pennsylvania State University/National Center for Atmospheric Research Mesoscale Model), and H. Zhang et al. (2012) using the WRF model. For O₃ in Beijing of the BTH region and Guangzhou of the PRD region, the NMB, NME and IOA were -22.80%, 58.70% and 0.79, respectively (Table 1 for case R), comparable to the values of 30.2% for NMB, 55.8% for NME and 0.91 for IOA reported in L. Li et al. (2012) using the CMAQ model. When HONO emissions, Reaction (R4) and the P_{unknown} were included, the NMB, NME and IOA increased to -2.20%, 66.10% and 0.80, respectively (Table 1 for case R_p). The NO₂ fluctuations were generally captured (Fig. 4) but the simulated amplitude of NO₂ was underestimated in some cases (Fig. 4). This underestimation could be related with the uncertainty of NO_x emissions. For NO₂ in case R, the NMB, NME and IOA were -13.50%, 42.10% and 0.57, respectively (Table 1), similar to the results of Wang et al. (2010) using the CMAQ model (NMB of -33.0%, NME of 50.0%, and IOA of 0.61). Compared with case R, NO₂ simulations (Table 1 for case R_p) were further underestimated for case R_p due to the underestimation of NO_x emissions in Guangzhou.

HONO simulations **only** with the gas-phase production (case R) were always substantially underestimated compared with observations (Fig. 5), similar to the results of Sarwar et al. (2008), Li et al. (2011) and An et al. (2013). When HONO

emissions and Reaction (R4) were included, HONO simulations were significantly improved, especially at night (Fig. 5 and Table 2 for case R_{wop}). For Beijing, the nighttime RMSE and NME were reduced by 0.90×10^6 molecules cm⁻³ and 44.70%, whereas the NMB and IOA were increased by 50.00% and 0.29, respectively (Table 2). For Guangzhou, the nighttime RMSE and NME were reduced by 0.44×10^6 molecules cm⁻³ and 32.90%, and the NMB and IOA were enhanced by 58.80% and 0.18, respectively. When the P_{unknown} was included, daytime HONO simulations were considerably improved (Fig. 5 and Table 2 for case R_p). Compared with case R_{wop}, the daytime NME in Beijing was reduced by 19.60%, and the NMB and IOA in Beijing were increased to -24.30% from -62.00% and 0.73 from 0.64, respectively (Table 2); the daytime NME in Guangzhou was reduced by 8.10%, and the NMB in Guangzhou was increased to -61.20% from -76.50% (Table 2).

Simulated diurnal variations of OH and HO₂ showed consistent patterns with the observed data (Fig. 6). When HONO emissions and Reaction (R4) were considered (case R_{wop}), OH and HO₂ enhancements were $\leq \sim 6\%$ in most cases compared with case R (Fig. 6 and Table 3), but the P_{unknown} led to 10%–150% improvements in OH simulations on 5–12 July 2006 (Fig. 6). The 20%–90% overestimation of OH mixing ratios on 20–25 July 2006 (Fig. 6) needs further investigation. Compared with case R, the NME was reduced by 79.60% ($=136.60\% - 57.00\%$), whereas the NMB was increased by 105.40% ($123.00\% - 17.60\%$), and the IOA was improved to 0.84 from 0.79 (Table 3). When the P_{unknown} was considered, HO₂ simulations were substantially improved (Fig. 6), the IOA was improved to 0.61 from 0.54 and the CC was improved to 0.66 from 0.57 (Table 3). However, HO₂ simulations were still substantially underestimated (Fig. 6). One of the major reasons for the HO₂ underestimation could be related to the considerable underestimation of anthropogenic volatile organic

compounds (VOCs) (Wang et al., 2014).

3.2 P_{unknown} simulations and its impacts on production and loss rates of HONO

High P_{unknown} values were found in the coastal regions of China (Fig. 7), especially in the BTH, YRD and PRD regions due to elevated emissions of NO_x (Zhang et al., 2009). The largest daytime average P_{unknown} value reached 2.5 ppb h^{-1} in Tianjin of the BTH region (Fig. 7a), whereas it was 2.0 ppb h^{-1} in Shanghai of the YRD region (Fig. 7b). The largest daytime average P_{unknown} value reached 1.2 ppb h^{-1} in Guangzhou and Shenzhen of the PRD (Fig. 7c), lower than the values of 2.5 ppb h^{-1} and 2.0 ppb h^{-1} . One major reason is the underestimation of daytime NO_2 mixing ratios in the PRD (Fig. 4b).

For case R, daytime HONO production was primarily from the reaction of OH and nitric oxide (NO) [Reaction (R1)], with a maximum production rate of 0.69 ppb h^{-1} in Beijing, 1.20 ppb h^{-1} in Shanghai, and 0.72 ppb h^{-1} in Guangzhou near noon due to high OH mixing ratios (Fig. 8a, c, e). The loss rate of HONO was 0.62 ppb h^{-1} in Beijing, 1.09 ppb h^{-1} in Shanghai, and 0.65 ppb h^{-1} in Guangzhou via Reaction (R2), much higher than the $0.01\text{--}0.02 \text{ ppb h}^{-1}$ in Beijing, Shanghai and Guangzhou via Reaction (R3) (Fig. 8b, d, f), indicating that Reaction (R2) accounted for approximately 99% of the total loss rate of HONO.

When the additional HONO sources [HONO emissions, Reaction (R4), and the P_{unknown}] were coupled into the WRF-Chem model, nighttime HONO was formed mainly via Reaction (R4) ($0.30\text{--}1.42 \text{ ppb h}^{-1}$ in Beijing, $0.20\text{--}0.45 \text{ ppb h}^{-1}$ in Shanghai, and $0.25\text{--}0.84 \text{ ppb h}^{-1}$ in Guangzhou) (Fig. 8a, c, e). HONO emissions contributed $0.04\text{--}0.62 \text{ ppb h}^{-1}$ to HONO production (Fig. 8a, c, e). Simulated P_{unknown} values ranged from 0.42 to 2.98 ppb h^{-1} in Beijing, from 0.18 to 2.58 ppb h^{-1} in Shanghai, and from 0.06 to 1.66 ppb h^{-1} in Guangzhou (Fig. 8a, c, e). The simulated

P_{unknown} values in Beijing (Fig. 8a) were in good agreement with the results of Spataro et al. (2013), with an average unknown daytime HONO production rate of 2.58 ppb h^{-1} in the studied summer period. However, the simulated P_{unknown} values in Guangzhou (Fig. 8e) were lower than the 2.36–4.90 ppb h^{-1} reported by Su et al (2008), due mainly to the underestimation of the daytime NO_2 mixing ratios in the PRD region. The additional HONO sources produce more HONO, which subsequently photolyzes to yield more OH. Therefore, the formation of HONO through Reaction (R1) was greatly enhanced, with a maximum of 4.70 [1.44 due to the P_{unknown}] ppb h^{-1} in Beijing, 4.25 [3.13] ppb h^{-1} in Shanghai, and 1.58 [0.40] ppb h^{-1} in Guangzhou in the morning (Fig. 8a, c, e), much higher than the 0.69 ppb h^{-1} in Beijing, 1.20 ppb h^{-1} in Shanghai, and 0.72 ppb h^{-1} in Guangzhou, respectively, for case R (Fig. 8a, c, e). Meanwhile, the loss rate of HONO via Reaction (R2) was significantly enhanced, with a maximum enhancement of 5.20 (= 5.82 – 0.62) [1.97 due to the P_{unknown}] ppb h^{-1} in Beijing, 4.31 (= 5.40 – 1.09) [1.44] ppb h^{-1} in Shanghai, and 1.96 (= 2.61 – 0.65) [1.18] ppb h^{-1} in Guangzhou (Fig. 8b, d, f). The HONO loss rate via dry deposition ranged from 0.28 to 0.45 ppb h^{-1} (not shown), roughly equivalent to the contribution of HONO emissions, suggesting that dry deposition of HONO cannot be neglected in high NO_x emission areas. The maximum P_{unknown} uncertainty range of 25% (Table S1), a 25% increase (decrease) in the slope factor (19.60) led to a 9.19%–18.62% increase (a 8.40%–14.32% decrease) in the maximum production and loss rate of HONO (Fig. S3).

3.3 P_{unknown} impacts on concentrations of OH, HO_2 and RO_2

Incorporation of the P_{unknown} into the WRF-Chem model led to substantial enhancements in the daytime average mixing ratios of OH in the coastal regions of China, e.g., 60%–190% in the BTH region, 60%–210% in the YRD region, and

60%–200% in the PRD region (Fig. 9a). The maximum enhancement of HO₂ reached 250% in the BTH region, 200% in the YRD region, and 140% in the PRD region (Fig. 9b). Similarly, a daytime average increase of 100%–180%, 60%–150% and 40%–80% in RO₂ [= CH₃O₂ (methylperoxy radical) + EHP (ethylperoxy radical) + C₂O₃ (peroxyacyl radical) + others] were found in the BTH, YRD and PRD regions, respectively (Fig. 9c).

Vertically, the P_{unknown} enhanced the monthly meridional-mean daytime (06:00–18:00 LST) mixing ratios of OH, HO₂ and RO₂ by 5%–38%, 5%–47% and 5%–48%, respectively, within 1000 m above the ground in the coastal regions of China (Fig. 10). Strong vertical mixing in the daytime in summer led to a roughly uniform vertical enhancement of OH, HO₂ and RO₂ within the 1000 m at the same latitude (Fig. 10). Different P_{unknown} values in different latitudes produced distinct differences in the enhancements of OH, HO₂ and RO₂, with a maximum located near 35°N (Fig. 10).

3.4 P_{unknown} impacts on the budgets of OH, HO₂ and RO₂

OH radicals are produced mainly through the reaction of HO₂ + NO, the photolysis of O₃ and HONO, and the reactions between O₃ and alkenes (Fig. 11). For case R, the predominant contribution to P(OH) (production rate of OH) was the reaction of HO₂ + NO (Fig. S1a, c, e), and the photolysis of O₃ was the second most important source of OH (Fig. S1a, c, e). When the three additional HONO sources were added, the most important source was the reaction of HO₂ + NO, with a diurnal maximum conversion rate reaching 9.38 [7.23 due to the P_{unknown}] ppb h⁻¹ in Beijing, 2.63 [1.15] ppb h⁻¹ in Shanghai, and 4.88 [1.43] ppb h⁻¹ in Guangzhou near noon (Fig. 11a, c, e). The photolysis of HONO became the second most important source of OH in Beijing and Guangzhou before 10:00 LST, and in Shanghai before 12:00 LST; the

diurnal peaks were 3.72 [3.06] ppb h⁻¹ in Beijing at 09:00 LST, 0.89 [0.62] ppb h⁻¹ in Shanghai at 11:00 LST, and 0.97 [0.78] ppb h⁻¹ in Guangzhou at 09:00 LST (Fig. 11a, c, e), which were comparable to or lower than the 3.10 ppb h⁻¹ reported by Elshorbany et al. (2009). Kanaya et al. (2009), who also conducted similar studies at Mount Tai (located in a rural area) of China, using an observationally constrained box model, suggested that the reaction of HO₂ + NO was the predominant OH source, with a daytime average of 3.72 ppb h⁻¹, more than the 1.38 ppb h⁻¹ of the photolysis of O₃. Using an observationally constrained box model, Hens et al. (2014) reported similar results in a boreal forest, in which the dominant contributor to OH was the reaction of HO₂ + NO, ranging from 0.23 to 1.02 ppb h⁻¹ during daytime. The production rates of OH in our study were higher than in Kanaya et al. (2009) and Hens et al. (2014) due to higher NO_x emissions in urban areas than in rural areas.

The dominant loss rate of OH was the reaction of OH + NO₂ for both cases R and R_p (Figs. 11b, d, f and S1b, d, f). The diurnal maximum loss rates were 1.98 ppb h⁻¹ in Beijing, 1.12 ppb h⁻¹ in Shanghai, and 1.70 ppb h⁻¹ in Guangzhou for case R (Fig. S1b, d, f), whereas these values were 5.61 [4.38 due to the P_{unknown}] ppb h⁻¹ in Beijing, 2.00 [1.00] ppb h⁻¹ in Shanghai, and 2.65 [1.02] ppb h⁻¹ in Guangzhou for case R_p (Fig. 11b, d, f). The reactions of OH + VOCs to form HO₂ and RO₂ were the second most important loss path of OH, with a diurnal maximum of 0.75–1.73 ppb h⁻¹ for case R (Fig. S1b, d, f) and 1.57 [0.82 due to the P_{unknown}] to 5.37 [4.05] ppb h⁻¹ for case R_p in Beijing, Shanghai and Guangzhou (Fig. 11b, d, f). The third most important OH loss path was the reaction of OH + CO to form HO₂; the diurnal maximum rates were 0.46–1.47 ppb h⁻¹ for case R (Fig. S1b, d, f) and 0.93 [0.49 due to the P_{unknown}] to 3.58 [2.86] ppb h⁻¹ for case R_p in Beijing, Shanghai and Guangzhou (Fig. 11b, d, f).

The averaged radical conversion rates in the daytime (06:00–18:00 LST) are

illustrated in Fig. 12. OH radicals are produced mainly via the photolysis of O₃, HONO and hydrogen peroxide (H₂O₂), and the reactions between O₃ and alkenes, after which OH radicals enter the RO_x (= OH + HO₂ + RO₂) cycle (Fig. 12 and Tables 4, S2 and S3).

For case R, the reaction of HO₂ + NO was the major source of OH [2.78 ppb h⁻¹ (81.73% of the total daytime average production rate of OH) in Beijing, 0.73 ppb h⁻¹ (67.09%) in Shanghai, and 1.75 ppb h⁻¹ (71.54%) in Guangzhou] (Fig. 12a and Table 4). The second largest source of OH was the photolysis of O₃ (Table 4). OH radicals were removed mainly through the reaction of OH + NO₂ [1.12 ppb h⁻¹ (39.31% of the total daytime average loss rate of OH) in Beijing, 0.47 ppb h⁻¹ (46.63%) in Shanghai, and 0.77 ppb h⁻¹ (38.33%) in Guangzhou] (Table 4), whereas those were converted to HO₂ mainly via the reaction of OH + CO (Table 4). For HO₂, the predominant production pathways were the reactions of OH + CO and CH₃O₂ + NO and the photolysis of formaldehyde (HCHO) (Table S2). HO₂ radicals were consumed primarily via the reaction of HO₂ + NO [2.78 ppb h⁻¹ (99.34%) in Beijing, 0.73 ppb h⁻¹ (99.61%) in Shanghai, and 1.75 ppb h⁻¹ (98.29%) in Guangzhou] (Table S2). RO₂ radicals were formed mainly from the reactions of OH + OLET (terminal olefin carbons)/OLEI (internal olefin carbons), OH + ETH (ethene), OH + methane (CH₄), and OH + AONE (acetone). RO₂ radicals were consumed primarily via the reaction of CH₃O₂ + NO [0.54 ppb h⁻¹ (94.56%) in Beijing, 0.16 ppb h⁻¹ (95.28%) in Shanghai, and 0.33 ppb h⁻¹ (96.07%) in Guangzhou] (Table S3).

When the three additional HONO sources were inserted into the WRF-Chem model (case R_p), the daytime average OH production rate was enhanced by 4.32 (= 7.10 - 2.78) [3.86 due to the P_{unknown}] ppb h⁻¹ in Beijing, 0.67 (= 1.40 - 0.73) [0.64] ppb h⁻¹ in Shanghai, and 0.80 (= 2.55 - 1.75) [0.68] ppb h⁻¹ in Guangzhou via the

reaction of $\text{HO}_2 + \text{NO}$, and by $1.86 [1.86] \text{ ppb h}^{-1}$ in Beijing, $0.50 [0.50] \text{ ppb h}^{-1}$ in
 Shanghai, and $0.49 [0.47] \text{ ppb h}^{-1}$ in Guangzhou via the photolysis of HONO,
 respectively (Table 4). The enhancements of the daytime average OH production rate
 due to the photolysis of HONO were comparable to or lower than the 2.20 ppb h^{-1}
 obtained by Liu et al. (2012). The daytime average OH loss rate was increased by
 $2.03 [1.92 \text{ due to the } P_{\text{unknown}}] \text{ ppb h}^{-1}$ in Beijing, $0.58 [0.55] \text{ ppb h}^{-1}$ in Shanghai, and
 $0.65 [0.58] \text{ ppb h}^{-1}$ in Guangzhou via the reaction of $\text{OH} + \text{NO}_2$, and by $1.78 [1.64]$
 ppb h^{-1} in Beijing, $0.31 [0.28] \text{ ppb h}^{-1}$ in Shanghai, and $0.42 [0.36] \text{ ppb h}^{-1}$ in
 Guangzhou via the reaction of $\text{OH} + \text{CO}$, respectively (Table 4). Similarly, the
 daytime average HO_2 production rate was increased by $0.31 [0.28 \text{ due to the } P_{\text{unknown}}]$
 to $1.78 [1.64] \text{ ppb h}^{-1}$ in Beijing, Shanghai and Guangzhou via the reaction of $\text{OH} +$
 CO , and by $0.63 [0.59] \text{ ppb h}^{-1}$ in Beijing, $0.10 [0.09] \text{ ppb h}^{-1}$ in Shanghai, and 0.19
 $[0.17] \text{ ppb h}^{-1}$ in Guangzhou via the reaction of $\text{CH}_3\text{O}_2 + \text{NO}$; whereas, the daytime
 average HO_2 loss rate was enhanced by $0.67 [0.61 \text{ due to the } P_{\text{unknown}}]$ to $4.32 [4.27]$
 ppb h^{-1} in Beijing, Shanghai and Guangzhou via the reaction of $\text{HO}_2 + \text{NO}$ (Table
 S2).

Overall, the **net** daytime production rate of RO_x was increased to $3.48 (= 2.56 +$
 $0.71 + 0.21) [2.06 \text{ due to the } P_{\text{unknown}}]$ from $1.20 (= 0.60 + 0.43 + 0.17) \text{ ppb h}^{-1}$ in
 Beijing, $1.09 (= 0.86 + 0.19 + 0.04) [0.45]$ from $0.54 (= 0.36 + 0.14 + 0.04) \text{ ppb h}^{-1}$ in
 Shanghai, and $1.52 (= 1.21 + 0.26 + 0.05) [0.58]$ from $0.92 (= 0.68 + 0.20 + 0.04) \text{ ppb}$
 h^{-1} in Guangzhou (Fig. 12) due to the **three** additional HONO sources, indicating that
 the RO_x source was mainly from OH production, especially via the photolysis of
 HONO (Tables 4, S2 and S3). This result is different from the conclusion of Liu et al.
 (2012) that the photolysis of HONO and oxygenated VOCs is the largest RO_x source.
 One of the primary reasons for this is the underestimation of anthropogenic VOCs

(Wang et al., 2014). For Beijing, the net production rate of RO_x was 3.48 ppb h^{-1} , lower than the 6.60 ppb h^{-1} from the field studies of Liu et al. (2012). Our results reconfirmed the view of Ma et al. (2012) that the North China Plain acts as an oxidation pool. The additional HONO sources produced an increase of $2.03 [1.96 \text{ due to the } P_{\text{unknown}}]$ ppb h^{-1} in Beijing, $0.56 [0.54] \text{ ppb h}^{-1}$ in Shanghai, and $0.66 [0.59] \text{ ppb h}^{-1}$ in Guangzhou in the net loss rate of RO_x (Fig. 12).

4. Conclusions

The relationship between the P_{unknown} , NO_2 mixing ratios and $J(\text{NO}_2)$ was investigated using available data from 13 field studies across the globe. The formula $P_{\text{unknown}} \approx 19.60[\text{NO}_2] \cdot J(\text{NO}_2)$ was obtained, and then the three additional HONO sources (i.e., the P_{unknown} , HONO emissions and nighttime hydrolysis conversion of NO_2 on aerosols) were inserted into the WRF-Chem model, to assess the P_{unknown} impacts on the concentrations and budgets of HONO and RO_x in the coastal regions of China. The results showed that:

(1) The additional HONO sources led to significant improvements in the simulations of HONO and OH, especially in the daytime.

(2) Elevated daytime average P_{unknown} values were found in the coastal regions of China, reaching 2.5 ppb h^{-1} in the BTH region, 2.0 ppb h^{-1} in the YRD region, and 1.2 ppb h^{-1} in the PRD region.

(3) The additional HONO sources substantially enhanced the production and loss rates of HONO. Dry deposition of HONO contributed $0.28\text{--}0.45 \text{ ppb h}^{-1}$ to the loss rate of HONO, approximately equivalent to the contribution of HONO emissions, emphasizing the importance of dry deposition of HONO in high NO_x emissions areas.

(4) The P_{unknown} produced a 60%–210% enhancement of OH, a 60%–250% enhancement of HO_2 , and a 60%–180% enhancement of RO_2 near the ground in the

major cities of the coastal regions of China. Vertically, the P_{unknown} enhanced the daytime meridional-mean mixing ratios of OH, HO₂ and RO₂ by 5%–38%, 5%–47% and 5%–48%, respectively, within 1000 m above the ground.

(5) When the three additional HONO sources were added, the photolysis of HONO became the second most important source of OH in Beijing and Guangzhou before 10:00 LST, and in Shanghai before 12:00 LST, with a maximum of 3.72 [3.06 due to the P_{unknown}] ppb h⁻¹ in Beijing, 0.89 [0.62] ppb h⁻¹ in Shanghai, and 0.97 [0.78] ppb h⁻¹ in Guangzhou; whereas, the reaction of HO₂ + NO was the most important source of OH, dominated in Beijing and Guangzhou after 10:00 LST and in Shanghai after 12:00 LST, with a maximum of 9.38 [7.23] ppb h⁻¹ in Beijing, 2.63 [1.15] ppb h⁻¹ in Shanghai, and 4.88 [1.43] ppb h⁻¹ in Guangzhou.

Overall, the above results suggest that the P_{unknown} significantly enhances the atmospheric oxidation capacity in the coastal regions of China by increasing RO_x concentrations and accelerating RO_x cycles, and could lead to considerable increases in concentrations of inorganic aerosols and secondary organic aerosols and further aggravate haze events in these regions.

Acknowledgements

This research was partially supported by the National Natural Science Foundation of China (41175105, 41405121), a Key Project of the Chinese Academy of Sciences (XDB05030301), and the Carbon and Nitrogen Cycle Project of the Institute of Atmospheric Physics, Chinese Academy of Sciences, and the Beijing Municipal Natural Science Foundation (8144054).

References

Acker, K., Mödler, D.: Corrigendum to: Atmospheric variation of nitrous acid at

524 different sites in Europe. *Environmental Chemistry*, 4(5), 364-364, 2007.

525 Acker, K., Möller, D., Wieprecht, W., Meixner, F. X., Bohn, B., Gilge, S.,
 526 Plass-Dülmer, C., and Berresheim, H.: Strong daytime production of OH from
 527 HNO₂ at a rural mountain site, *Geophys. Res. Lett.*, 33(2), doi:
 528 10.1029/2005GL024643, 2006.

529 Alicke, B., Platt, U., and Stutz, J.: Impact of nitrous acid photolysis on the total
 530 hydroxyl radical budget during the limitation of oxidant production/Pianura
 531 padana produzione di ozono study in Milan, J. *Geophys. Res. –Atmos.*,
 532 107(D22): LOP9-1 – LOP9-17, doi: 10.1029/2000JD000075, 2002.

533 Amedro, D., Parker, A. E., Schoemaeker, C., Fittschen, C.: Direct observation of OH
 534 radicals after 565nm multi-photon excitation of NO₂ in the presence of H₂O.
 535 *Chemical Physics Letters*, 513(1), 12-16, 2011.

536 Ammann, M., Kalberer, M., Jost, D. T., Tobler, L., Rössler, E., Piguet, D., Gägeler,
 537 H., Baltensperger, U.: Heterogeneous production of nitrous acid on soot in
 538 polluted air masses. *Nature*, 395(6698), 157-160, 1998.

539 An, J., Li, Y., Wang, F., and Xie, P.: Impacts of photoexcited NO₂ chemistry and
 540 heterogeneous reactions on concentrations of O₃ and NO_y in Beijing, Tianjin and
 541 Hebei province of China, *Air Quality-Models and Applications*, Prof. Dragana
 542 Popovic (Ed.), InTech, ISBN: 978-953-307-307-1, doi: 10.5772/16858, 2011.

543 An, J., Li, Y., Chen, Y., Li, J., Qu, Y., Tang, Y.: Enhancements of major aerosol
 544 components due to additional HONO sources in the North China Plain and
 545 implications for visibility and haze. *Advances in Atmospheric Science*, 30, 57-66,
 546 2013.

547 Atkinson, R., Aschmann, S. M.: Hydroxyl radical production from the gas-phase
 548 reactions of ozone with a series of alkenes under atmospheric

549 conditions. Environmental science & technology, 27(7), 1357-1363, 1993.

550 Carr, S., Heard, D., Blitz, M.: Comment on “Atmospheric Hydroxyl Radical
551 Production from Electronically Excited NO₂ and H₂O”. Science, 324, 5925,
552 doi:10.1126/science.1166669, 2009.

553 Crutzen, P. J., Zimmermann, P. H.: The changing photochemistry of the
554 troposphere. Tellus B, 43(4), 136-151, 1991.

555 Czader, B. H., Rappenglück, B., Percell, P., Byun, D. W., Ngan, F., Kim, S.:
556 Modeling nitrous acid and its impact on ozone and hydroxyl radical during the
557 Texas Air Quality Study 2006. Atmospheric Chemistry and Physics, 12(15),
558 6939-6951, 2012.

559 Dentener, F. J., Crutzen, P. J.: Reaction of N₂O₅ on tropospheric aerosols: Impact on
560 the global distributions of NO_x, O₃, and OH. Journal of Geophysical Research:
561 Atmospheres (1984–2012), 98(D4), 7149-7163, 1993.

562 Elshorbany, Y. F., Kurtenbach, R., Wiesen, P., Lissi, E., Rubio, M., Villena, G.,
563 Gramsch, E., Rickard, A. R., Pilling, M. J., Kleffmann, J.: Oxidation capacity of
564 the city air of Santiago, Chile. Atmospheric Chemistry and Physics, 9(6),
565 2257-2273, 2009.

566 Emmons, L. K., Walters, S., Hess, P. G., Lamarque, J. F., Pfister, G. G., Fillmore, D.,
567 Granier, C., Guenther, A., Kinnison, D., Laepple, T., Orlando, J., Tie, X.,
568 Tyndall, G., Wiedinmyer, C., Baughcum, S. L., Kloster, S.: Description and
569 evaluation of the Model for Ozone and Related chemical Tracers, version 4
570 (MOZART-4). Geoscientific Model Development, 3(1), 43-67, 2010.

571 Fast, J. D., Gustafson, W. I., Easter, R. C., Zaveri, R. A., Barnard, J. C., Chapman, E.
572 G., Grell, G. A., and Peckham, S. E.: Evolution of ozone, particulates, and
573 aerosol direct radiative forcing in the vicinity of Houston using a fully coupled

574 meteorology chemistry aerosol model, J. Geophys. Res. –Atmos., 111(D21), doi:
575 10.1029/2005JD006721, 2006.

576 Finlayson-Pitts, B. J., Wingen, L. M., Sumner, A. L., Syomin, D., Ramazan, K. A.:
577 The heterogeneous hydrolysis of NO₂ in laboratory systems and in outdoor and
578 indoor atmospheres: An integrated mechanism. *Physical Chemistry Chemical*
579 *Physics*, 5(2), 223-242, 2003.

580 Fried, A., McKeen, S., Sewell, S., Harder, J., Henry, B., Goldan, P., Kuster, W.,
581 William, E., Baumann, K., Shett, R., Cantrell, C.: Photochemistry of
582 formaldehyde during the 1993 Tropospheric OH Photochemistry
583 Experiment. *Journal of Geophysical Research: Atmospheres*
584 (1984–2012), 102(D5), 6283-6296, 1997.

585 George, C., Strekowski, R. S., Kleffmann, J., Stemmler, K., Ammann, M.:
586 Photoenhanced uptake of gaseous NO₂ on solid organic compounds: a
587 photochemical source of HONO?. *Faraday discussions*, 130, 195-210, 2005.

588 Gonçalves, M., Dabdub, D., Chang, W. L., Jorba, O., Baldasano, J. M.: Impact of
589 HONO sources on the performance of mesoscale air quality models.
590 *Atmospheric Environment*, 54, 168-176, 2012.

591 Grell, G. A., Peckham, S. E., Schmitz, R., McKeen, S. A., Frost, G., Skamarock, W.
592 C., Eder, B.: Fully coupled “online” chemistry within the WRF model.
593 *Atmospheric Environment*, 39(37), 6957-6975, 2005.

594 Hens, K., Novelli, A., Martinez, M., Auld, J., Axinte, R., Bohn, B., Fischer, H.,
595 Keronen, P., Kubistin, D., Nödscher, A. C., Oswald, R., Paasonen, P., Petäjä T.,
596 Regelin, E., Sander, R., Sinha, V., Sipilä M., Taraborrelli, D., Tatum Ernest, C.,
597 Williams, J., Lelieveld, J., Harder, H.: Observation and modeling of HO_x radicals
598 in a boreal forest. *Atmospheric Chemistry and Physics*, 14, 8723–8747, 2014.

599 Jacob, D. J.: Heterogeneous chemistry and tropospheric ozone. *Atmospheric*
 600 *Environment*, 34(12), 2131-2159, 2000.

601 Kanaya, Y., Pochanart, P., Liu, Y., Li, J., Tanimoto, H., Kato, S., Suthawaree, J.,
 602 Inomata, S., Taketani, F., Okuzawa, K., Kawamura, K., Akimoto, H., Wang, Z.
 603 F.: Rates and regimes of photochemical ozone production over Central East
 604 China in June 2006: a box model analysis using comprehensive measurements of
 605 ozone precursors. *Atmospheric Chemistry and Physics*, 9, 7711–7723, 2009.

606 Kerbrat, M., Legrand, M., Preunkert, S., Gallée, H., and Kleffmann, J.: Nitrous acid at
 607 Concordia (inland site) and Dumont d’Urville (coastal site), East Antarctica, *J.*
 608 *Geophys. Res. –Atmos.*, 117(D8), doi: 10.1029/2011JD017149, 2012.

609 Kleffmann, J., Gavriloaiei, T., Hofzumahaus, A., Holland, F., Koppmann, R., Rupp,
 610 L., Schlosser, E., Siese, M., and Wahner, A.: Daytime formation of nitrous acid: a
 611 major source of OH radicals in a forest, *J. Geophys. Res. Lett.*, 32(5), doi:
 612 10.1029/2005GL022524, 2005.

613 Kleffmann, J., Gavriloaiei, T., Hofzumahaus, A., Holland, F., Koppmann, R., Rupp,
 614 L., Schlosser, E., Siese, M., Wahner, A.: Daytime formation of nitrous acid: A
 615 major source of OH radicals in a forest. *Geophysical Research Letters*, 32(5),
 616 2005.

617 Li, G., Lei, W., Zavala, M., Volkamer, R., Dusanter, S., Stevens, P., Molina, L. T.:
 618 Impacts of HONO sources on the photochemistry in Mexico City during the
 619 MCMA-2006/MILAGO Campaign. *Atmospheric Chemistry and Physics*, 10,
 620 6551–6567, 2010.

621 Li, L., Chen, C. H., Huang, C., Huang, H. Y., Zhang, G. F., Wang, Y. J., Wang,
 622 H. L., Lou, S. R., Qiao, L. P., Zhou, M., Chen, M. H., Chen, Y. R., Fu,
 623 J. S., Streets, D. G., Jang, C. J.: Process analysis of regional ozone formation

624 over the Yangtze River Delta, China using the Community Multi-scale Air
625 Quality modeling system. *Atmospheric Chemistry and Physics*, 12, 10971-10987,
626 2012.

627 Li, S., J. Matthews, and A. Sinha.: Atmospheric hydroxyl radical production from
628 electronically excited NO₂ and H₂O. *Science*, 319, 1657–1660, 2008.

629 Li, X., Brauers, T., Häseler, R., Bohn, B., Fuchs, H., Hofzumahaus, A., Holland, F.,
630 Lou, S., Lu, K. D., Rohrer, F., Hu, M., Zeng, L. M., Zhang, Y. H., Garland, R.
631 M., Su, H., Nowak, A., Wiedensohler, A., Takegawa, N., Shao, M., Wahner, A.:
632 Exploring the atmospheric chemistry of nitrous acid (HONO) at a rural site in
633 Southern China. *Atmospheric Chemistry and Physics*, 12(3), 1497-1513, 2012.

634 Li, Y., An, J., Min, M., Zhang, W., Wang, F., Xie, P.: Impacts of HONO sources on
635 the air quality in Beijing, Tianjin and Hebei Province of China. *Atmospheric*
636 *Environment*, 45(27), 4735-4744, 2011.

637 Liu, Z., Wang, Y., Gu, D., Zhao, C., Huey, L. G., Sticke, R., Liao, J., Shao, M., Zhu,
638 T., Zeng, L., Amoroso, A., Costabile, F., Chang, C.-C., Liu, S.-C.: Summertime
639 photochemistry during CARE Beijing-2007: RO_x budgets and O₃ formation.
640 *Atmospheric Chemistry and Physics*, 12, 7737–7752, 2012.

641 Lu, K. D., Rohrer, F., Holland, F., Fuchs, H., Bohn, B., Brauers, T., Chang, C. C.,
642 Haseler, R., Hu, M., Kita, K., Kondo, Y., Li, X., Lou, S. R., Nehr, S., Shao, M.,
643 Zeng, L. M., Wahner, A., Zhang, Y. H., Hofzumahaus, A.: Observation and
644 modelling of OH and HO₂ concentrations in the Pearl River Delta 2006: a
645 missing OH source in a VOC rich atmosphere. *Atmospheric Chemistry and*
646 *Physics*, 12(3), 1541-1569, 2012.

647 Ma, J. Z., Wang, W., Chen, Y., Liu, H. J., Yan, P., Ding, G. A., Wang, M. L., Sun, J.,
648 Lelieveld, J.: The IPAC-NC field campaign: a pollution and oxidization pool in

649 the lower atmosphere over Huabei, China. *Atmospheric Chemistry and Physics*,
650 12, 3883–3908, 2012.

651 Michoud, V., Colomb, A., Borbon, A., Miet, K., Beekmann, M., Camredon, M.,
652 Aumont, B., Perrier, S., Zapf, P., Siour, G., Ait-Helal, W., Afif, C., Kukui, A.,
653 Furger, M., Dupont, J. C., Haeffelin, M., Doussin, J. F.: Study of the unknown
654 HONO daytime source at a European suburban site during the MEGAPOLI
655 summer and winter field campaigns. *Atmospheric Chemistry and Physics*, 14(6),
656 2805-2822, 2014.

657 Monge, M. E., D’Anna, B., Mazri, L., Giroir-Fendler, A., Ammann, M., Donaldson,
658 D. J., George, C.: Light changes the atmospheric reactivity of soot. *Proceedings*
659 *of the National Academy of Sciences*, 107(15), 6605-6609, 2010.

660 Oswald, R., Behrendt, T., Ermel, M., Wu, D., Su, H., Cheng, Y., Breuninger, C.,
661 Moravek, A., Mougin, E., Delon, C., Loubet, B., Pommerening-Röser, A., Sörgel,
662 M., Pöschl, U., Hoffmann, T., Andreae, M.O., Meixner, F.X., Trebs, I.: HONO
663 emissions from soil bacteria as a major source of atmospheric reactive nitrogen.
664 *Science* 341, 1233-1235, 2013.

665 Paulson, S. E., Sen, A. D., Liu, P., Fenske, J. D., Fox, M. J.: Evidence for formation
666 of OH radicals from the reaction of O₃ with alkenes in the gas
667 phase. *Geophysical research letters*, 24(24), 3193-3196, 1997.

668 Platt, U., Perner, D., Harris, G. W., Winer, A. M., Pitts, J. N.: Observations of nitrous
669 acid in an urban atmosphere by differential optical absorption. *Nature* 285,
670 312-314 (29 May 1980); doi: 10.1038/285312a0, 1980.

671 Qin, M., Xie, P. H., Liu, W. Q., Li, A., Dou, K., Fang, W., Liu, J., Zhang, W. J.:
672 Observation of atmospheric nitrous acid with DOAS in Beijing, China. *Journal*
673 *of Environmental Sciences*, 18(1), 69-75, 2006.

674 Qin, M., Xie, P., Su, H., Gu, J., Peng, F., Li, S., Zengb, L., Liua, J., Liua W., Zhang,
 675 Y.: An observational study of the HONO–NO₂ coupling at an urban site in
 676 Guangzhou City, South China. *Atmospheric Environment*, 43(36), 5731-5742,
 677 2009.

678 Ren, X., Gao, H., Zhou, X., Crounse, J. D., Wennberg, P. O., Browne, E. C.,
 679 LaFranchi, B. W., Cohen, R. C., McKay, M., Goldstein, A. H., Mao, J.:
 680 Measurement of atmospheric nitrous acid at Bodgett Forest during
 681 BEARPEX2007. *Atmospheric Chemistry and Physics*, 10(13), 6283-6294, 2010.

682 Ren, X., Harder, H., Martinez, M., Leshner, R. L., Oliger, A., Simpasa, J. B., Brunea, W.
 683 H., Schwab, J. J., Demerjian, K. L., He, Y., Zhou, X., Gao, H.: OH and HO₂
 684 Chemistry in the urban atmosphere of New York City. *Atmospheric*
 685 *Environment*, 37(26), 3639-3651, 2003.

686 Ren, X., Sanders, J. E., Rajendran, A., Weber, R. J., Goldstein, A.H., Pusede, S. E.,
 687 Browne, E. C., Min, K.-E., and Cohen, R.C.: A relaxed eddy accumulation
 688 system for measuring vertical fluxes of nitrous acid, *Atmos. Meas. Tech.*, 4,
 689 2093–2103, doi:10.5194/amt-4-2093-2011, 2011.

690 Rohrer, F., Bohn, B., Brauers, T., Brüning, D., Johnen, F. J., Wahner, A., Kleffmann,
 691 J.: Characterisation of the photolytic HONO-source in the atmosphere simulation
 692 chamber SAPHIR. *Atmospheric Chemistry and Physics*, 5(8), 2189-2201, 2005.

693 Sörgel, M., Regelin, E., Bozem, H., Diesch, J. M., Drewnick, F., Fischer, H., Harder,
 694 H., Held, A., Hosaynali-Beygi, Z., Martinez, M., Zetzsch, C.: Quantification of
 695 the unknown HONO daytime source and its relation to NO₂. *Atmospheric*
 696 *Chemistry and Physics*, 11(20), 10433-10447, 2011.

697 Sarwar, G., Roselle, S. J., Mathur, R., Appel, W., Dennis, R. L., Vogel, B.: A
 698 comparison of CMAQ HONO predictions with observations from the Northeast

699 Oxidant and Particle Study. *Atmospheric Environment*, 42(23), 5760-5770,
700 2008.

701 Spataro, F., Ianniello, A., Esposito, G., Allegrini, I., Zhu, T., Hu, M.: Occurrence of
702 atmospheric nitrous acid in the urban area of Beijing (China). *Science of the Total*
703 *Environment*, 447, 210-224, 2013.

704 Stemmler, K., Ammann, M., Donders, C., Kleffmann, J., George, C.: Photosensitized
705 reduction of nitrogen dioxide on humic acid as a source of nitrous acid. *Nature*,
706 440(7081), 195-198, 2006.

707 Stemmler, K., Ndour, M., Elshorbany, Y., Kleffmann, J., D'anna, B., George,
708 C., Bohn, B., Ammann, M.: Light induced conversion of nitrogen dioxide into
709 nitrous acid on submicron humic acid aerosol. *Atmospheric Chemistry and*
710 *Physics*, 7(16), 4237-4248, 2007.

711 Stone, D., Whalley, L. K., Heard, D. E.: Tropospheric OH and HO₂ radicals: field
712 measurements and model comparisons. *Chemical Society Reviews*, 41,
713 6348-6404, 2012.

714 Su, H., Cheng, Y., Oswald, R., Behrendt, T., Trebs, I., Meixner, F. X., Andreae, M.
715 O., Cheng, P., Zhang, Y., Pöschl, U.: Soil nitrite as a source of atmospheric
716 HONO and OH radicals. *Science*, 333(6049), 1616-1618, 2011.

717 Su, H., Cheng, Y. F., Shao, M., Gao, D. F., Yu, Z. Y., Zeng, L. M., Slanina, J., Zhang,
718 Y. H., and Wiedensohler, A.: Nitrous acid (HONO) and its daytime sources at a
719 rural site during the 2004 PRIDE-PRD experiment in China, *J. Geophys. Res.*
720 *–Atmos.*, 113(D14), doi: 10.1029/2007JD009060, 2008.

721 Tang, Y., An, J., Li, Y., Wang, F.: Uncertainty in the uptake coefficient for HONO
722 formation on soot and its impacts on concentrations of major chemical
723 components in the Beijing–Tianjin–Hebei region. *Atmospheric Environment*, 84,

724 163-171, 2014.

725 VandenBoer, T. C., Brown, S. S., Murphy, J. G., Keene, W. C., Young, C. J., Pszenny,
726 A. A. P., Kim, S., Warneke, C., de Gouw, J. A., Maben, J. R., Wagner, N. L.,
727 Riedel, T. P., Thornton, J. A., Wolfe, D. E., Dubé W. P., Öztürk, F., Brock, C.
728 A., Grossberg, N., Lefer, B., Lerner, B. Middlebrook, A. M., Roberts, J. M.:
729 Understanding the role of the ground surface in HONO vertical structure: High
730 resolution vertical profiles during NACHTT-11. *Journal of Geophysical*
731 *Research: Atmospheres*, 118, 10,155–10,171, doi:10.1002/jgrd.50721, 2013.

732 Villena, G., Wiesen, P., Cantrell, C. A., Flocke, F., Fried, A., Hall, S. R., Hornbrook, R.
733 S., Knapp, D., Kosciuch, E., Mauldin, R. L., McGrath, J. A., Montzka, D.,
734 Richter, D., Ullmann, K., Walega, J., Weibring, P., Weinheimer, A., Staebler, R.
735 M., Liao, J., Huey, L. G., and Kleffmann, J.: Nitrous acid (HONO) during polar
736 spring in Barrow, Alaska: a net source of OH radicals?, *J. Geophys. Res.*
737 *–Atmos.*, 116(D14), doi: 10.1029/2011JD016643, 2011.

738 Wang, F., An, J., Li, Y., Tang, Y., Lin, J., Qu, Y., Cheng, Y., Zhang, B., Zhai, J.:
739 Impacts of Uncertainty in AVOC Emissions on the Summer RO_x Budget and
740 Ozone Production Rate in the Three Most Rapidly-Developing Economic
741 Growth Regions of China. *Advances in Atmospheric Sciences*, 31, 1331–1342,
742 2014.

743 Wang, X., Zhang, Y., Hu, Y., Zhou, W., Lu, K., Zhong, L., Zeng, L., Shao, M., Hu,
744 M., Russell, A. G.: Process analysis and sensitivity study of regional ozone
745 formation over the Pearl River Delta, China, during the PRIDE-PRD2004
746 campaign using the Community Multiscale Air Quality modeling
747 system. *Atmospheric Chemistry and Physics*, 10(9), 4423-4437, 2010.

748 Wong, K. W., Oh, H. J., Lefer, B. L., Rappenglück, B., Stutz, J.: Vertical profiles of

749 nitrous acid in the nocturnal urban atmosphere of Houston, TX. *Atmospheric*
750 *Chemistry and Physics*, 11(8), 3595-3609, 2011.

751 Wong, K. W., Tsai, C., Lefer, B., Grossberg, N., Stutz, J.: Modeling of daytime
752 HONO vertical gradients during SHARP 2009. *Atmospheric Chemistry and*
753 *Physics*, 13(7), 3587-3601, 2013.

754 Wong, K. W., Tsai, C., Lefer, B., Haman, C., Grossberg, N., Brune, W. H., Ren,
755 X., Luke, W., Stutz, J.: Daytime HONO vertical gradients during SHARP 2009
756 in Houston, TX. *Atmospheric Chemistry and Physics*, 12(2), 635-652, 2012.

757 Wu, J., Xu, Z., Xue, L., Wang, T.: Daytime nitrous acid at a polluted suburban site in
758 Hong Kong: Indication of heterogeneous production on aerosol. *Proceedings of*
759 *12th international conference on atmospheric sciences and applications to air*
760 *quality*, Seoul, Korea, June 3-5, 2013, p. 52, 2013.

761 Zaveri, R. A., Peters, L. K.: A new lumped structure photochemical mechanism for
762 large - scale applications. *Journal of Geophysical Research: Atmospheres* (1984
763 - 2012), 104(D23), 30387-30415, 1999.

764 Zaveri, R. A., Easter, R. C., Fast, J. D., and Peters, L. K.: Model for simulating
765 aerosol interactions and chemistry (MOSAIC), *J. Geophys. Res. –Atmos.*,
766 113(D13), doi: 10.1029/2007JD008782, 2008.

767 Zhang, B., Tao, F.: Direct homogeneous nucleation of NO₂, H₂O, and NH₃ for the
768 production of ammonium nitrate particles and HONO gas. *Chemical Physics*
769 *Letters*, 489, 4-6, 143, 2010.

770 Zhang, H., Li, J., Ying, Q., Yu, J. Z., Wu, D., Cheng, Y., Kebin Hed, Jiang, J.: Source
771 apportionment of PM_{2.5} nitrate and sulfate in China using a source-oriented
772 chemical transport model. *Atmospheric Environment*, 62, 228-242, 2012.

773 Zhang, N., Zhou, X., Bertman, S., Tang, D., Alaghmand, M., Shepson, P. B., Carroll,

774 M. A.: Measurements of ambient HONO concentrations and vertical HONO flux
 775 above a northern Michigan forest canopy. *Atmospheric Chemistry and Physics*,
 776 12(17), 8285-8296, 2012.

777 Zhang, Q., Streets, D. G., Carmichael, G. R., He, K., Huo, H., Kannari, A., Klimont,
 778 Z., Park, I., Reddy, S., Fu, J. S., Chen, D., Duan, L., Lei, Y., Wang, L., Yao, Z.:
 779 Asian emissions in 2006 for the NASA INTEX-B mission. *Atmospheric*
 780 *Chemistry and Physics*, 9, 5131-5153, 2009.

781 Zhou, X., Civerolo, K., Dai, H., Huang, G., Schwab, J., and Demerjian, K:
 782 Summertime nitrous acid chemistry in the atmospheric boundary layer at a rural
 783 site in New York State, *J. Geophys. Res. –Atmos.*, 107(D21), ACH13-1 –
 784 ACH13-11, doi: 10.1029/2001JD001539, 2002a.

785 Zhou, X., Gao, H., He, Y., Huang, G., Bertman, S. B., Civerolo, K., and Schwab, J.:
 786 Nitric acid photolysis on surfaces in low-NO_x environments: significant
 787 atmospheric implications, *Geophys. Res. Lett.*, 30(23), doi:
 788 10.1029/2003GL018620, 2003.

789 Zhou, X., He, Y., Huang, G., Thornberry, T. D., Carroll, M. A., and Bertman, S. B.:
 790 Photochemical production of nitrous acid on glass sample manifold surface,
 791 *Geophys. Res. Lett.*, 29, 26-1 – 26-4, doi: 10.1029/2002GL015080, 2002b.

792 Zhou, X., Zhang, N., TerAvest, M., Tang, D., Hou, J., Bertman, S., Alaghmand, M.,
 793 Shepson, P. B. Carroll, M. A. Griffith, S., Dusanter, S., Stevens, P. S.: Nitric acid
 794 photolysis on forest canopy surface as a source for tropospheric nitrous acid.
 795 *Nature Geoscience*, 4(7), 440-443, 2011.

796 Table 1. Model performance statistics for O₃ and NO₂ in Beijing in August 2007 and Guangzhou in July 2006.

Species	Case	MB (ppb)	ME (ppb)	RMSE (ppb)	NMB (%)	NME (%)	IOA
O ₃	R _p	−0.65	19.40	25.44	−2.20	66.10	0.80
	R	−6.69	17.21	25.24	−22.80	58.70	0.79
NO ₂	R _p	−9.50	17.31	21.40	−29.10	53.00	0.51
	R	−4.40	13.75	17.61	−13.50	42.10	0.57

797 MB: mean bias; ME: mean error; RMSE: root-mean-square error; NMB: normalized mean bias; NME: normalized mean error; IOA: index of
798 agreement.

799

800

801

802

803

804

805

806

807 Table 2. Model performance statistics for daytime (06:00–18:00 LST) and nighttime (19:00–05:00 LST) HONO in Beijing in August 2007 and
808 Guangzhou in July 2006.

Species	Case	MB (10 ⁶ molec cm ⁻³)	ME (10 ⁶ molec cm ⁻³)	RMSE (10 ⁶ molec cm ⁻³)	NMB (%)	NME (%)	IOA	CC
HONO _{daytime} (Beijing)	R _p	-0.54	0.98	1.41	-24.30	44.50	0.73	0.57
	R _{wop}	-1.37	1.41	1.83	-62.00	64.10	0.64	0.63
	R	-2.07	2.07	2.58	-93.80	93.80	0.46	0.31
HONO _{nighttime} (Beijing)	R _p	-0.73	0.84	1.09	-42.20	49.10	0.77	0.74
	R _{wop}	-0.82	0.91	1.16	-47.90	53.20	0.75	0.75
	R	-1.68	1.68	2.06	-97.90	97.90	0.46	0.76
HONO _{daytime} (Guangzhou)	R _p	-0.38	0.43	0.58	-61.20	69.60	0.58	0.56
	R _{wop}	-0.48	0.49	0.65	-76.50	77.70	0.55	0.56
	R	-0.60	0.60	0.80	-95.60	96.20	0.43	-0.30
HONO _{nighttime} (Guangzhou)	R _p	-0.42	0.75	1.05	-32.90	58.50	0.66	0.43
	R _{wop}	-0.49	0.83	1.15	-38.40	64.30	0.63	0.38
	R	-1.25	1.25	1.59	-97.20	97.20	0.45	-0.01

809 CC: correlation coefficient.

810 Table 3. Model performance statistics for OH and HO₂ in Guangzhou in July 2006.

Species	Case	MB (10 ⁶ molec cm ⁻³)	ME (10 ⁶ molec cm ⁻³)	RMSE (10 ⁶ molec cm ⁻³)	NMB (%)	NME (%)	IOA	CC
OH	R _p	-1.35	4.37	6.22	-17.60	57.00	0.84	0.75
	R _{wop}	-3.00	4.58	6.25	-112.20	126.50	0.81	0.72
	R	-3.36	4.85	6.55	-123.00	136.60	0.79	0.70
HO ₂	R _p	-3.80	3.81	5.59	-78.50	78.60	0.61	0.66
	R _{wop}	-4.19	4.20	6.14	-86.60	86.70	0.54	0.59
	R	-4.22	4.23	6.16	-87.20	87.30	0.54	0.57

818 Table 4. Daytime (06:00–18:00 LST) average OH budgets in Beijing/Shanghai/Guangzhou in August 2007.
819

Reaction	Case R		Case R _{wop}		Case R _p	
	Rate (ppb h ⁻¹)	Contribution (%)	Rate (ppb h ⁻¹)	Contribution (%)	Rate (ppb h ⁻¹)	Contribution (%)
OH production						
HO₂+NO	2.778/0.732/1.748	81.73/67.09/71.54	3.242/0.760/1.871	83.74/68.00/72.02	7.101/1.402/2.553	73.34/61.95/67.55
* (HONO+hν)_{net}	--/--/--	--/--/--	--/--/0.017	--/--/0.66	1.855/0.497/0.489	19.16/21.98/12.93
O¹D+H₂O	0.465/0.307/0.617	13.68/28.17/25.27	0.479/0.306/0.630	12.36/27.38/24.24	0.568/0.312/0.651	5.86/13.80/17.23
O ₃ +OLET/OLEI	0.101/0.024/0.027	2.98/2.16/1.11	0.095/0.023/0.027	2.45/2.08/1.03	0.080/0.021/0.025	0.83/0.91/0.65
* (H₂O₂+hν)_{net}	0.035/0.023/0.029	1.02/2.07/1.17	0.035/0.023/0.030	0.91/2.03/1.16	0.037/0.022/0.032	0.38/0.97/0.19
HO ₂ +O ₃	0.009/0.001/0.014	0.28/0.07/0.59	0.010/0.001/0.015	0.26/0.06/0.58	0.026/0.001/0.019	0.27/0.05/0.51
* (HNO₃+hν)_{net}	0.005/0.001/0.002	0.15/0.06/0.10	0.005/0.001/0.002	0.13/0.06/0.09	0.007/0.001/0.003	0.07/0.04/0.07
ROOH+hν	0.003/0.004/0.005	0.09/0.36/0.19	0.003/0.004/0.005	0.09/0.38/0.19	0.007/0.007/0.007	0.07/0.29/0.19
O ₃ +ETH	0.002/<0.001/<0.001	0.05/0.02/0.01	0.002/<0.001/<0.001	0.04/0.02/0.01	0.001/<0.001/<0.001	0.02/0.01/0.01
HO ₂ +NO ₃	<0.001/<0.001/<0.001	<0.01/<0.01/0.01	<0.001/<0.001/<0.001	<0.01/<0.01/<0.01	<0.001/<0.001/<0.001	<0.01/<0.01/<0.01
O ₃ +ISOP	<0.001/<0.001/<0.001	0.01/<0.01/<0.01	<0.001/<0.001/<0.001	0.01/<0.01/<0.01	<0.001/<0.001/<0.001	<0.01/<0.01/<0.01
Total	3.399/1.091/2.443	100/100/100	3.873/1.118/2.598	100/100/100	9.683/2.263/3.779	100/100/100
OH loss						
OH+NO₂	1.116/0.474/0.770	39.31/46.63/38.33	1.225/0.501/0.844	38.11/45.86/38.86	3.146/1.045/1.424	38.08/44.29/40.76
OH+CO	0.785/0.203/0.576	27.65/19.97/28.67	0.932/0.227/0.637	29.00/20.78/29.33	2.573/0.506/1.001	31.14/21.45/28.65
OH+OLET/OLEI	0.192/0.054/0.059	6.76/5.31/2.94	0.264/0.065/0.077	8.21/5.95/3.55	0.537/0.206/0.095	6.50/8.73/2.72
OH+HCHO	0.150/0.050/0.146	5.28/4.92/7.27	0.166/0.053/0.156	5.16/4.85/7.18	0.544/0.096/0.242	6.59/4.07/6.93
OH+CH ₄	0.103/0.057/0.135	3.63/5.61/6.72	0.109/0.059/0.142	3.39/5.40/6.54	0.260/0.115/0.223	3.15/4.87/6.38
OH+ALD2/MGLY/AN OE	0.092/0.018/0.045	3.24/1.77/2.24	0.109/0.020/0.049	3.39/1.83/2.26	0.323/0.047/0.081	3.91/1.99/2.32
OH+SO ₂	0.054/0.030/0.035	1.90/2.95/1.74	0.064/0.034/0.041	1.99/3.11/1.89	0.172/0.116/0.072	2.08/4.92/2.06

OH+XYL	0.052/0.022/0.023	1.83/2.16/1.14	0.066/0.026/0.029	2.05/2.38/1.34	0.141/0.078/0.045	1.71/3.31/1.29
OH+H ₂	0.038/0.021/0.050	1.34/2.07/2.49	0.040/0.022/0.052	1.24/2.01/2.39	0.095/0.027/0.075	1.15/1.14/2.15
OH+TOL	0.027/0.007/0.011	0.95/0.69/0.55	0.034/0.008/0.014	1.06/0.73/0.64	0.086/0.025/0.024	1.04/1.06/0.69
OH+HONO	0.003/0.003/0.005	0.11/0.30/0.25	0.006/0.004/0.007	0.19/0.37/0.32	0.069/0.023/0.032	0.84/0.97/0.92
OH+HNO _x	0.005/0.001/0.005	0.18/0.10/0.25	0.005/0.001/0.005	0.16/0.09/0.23	0.015/0.002/0.008	0.18/0.08/0.23
OH+O ₃	0.028/0.006/0.035	0.99/0.59/1.70	0.029/0.006/0.036	0.90/0.55/1.66	0.072/0.005/0.046	0.87/0.21/1.32
OH+H ₂ O ₂	0.015/0.008/0.027	0.53/0.79/1.34	0.016/0.008/0.029	0.50/0.73/1.34	0.040/0.010/0.043	0.48/0.42/1.23
OH+ETH/OPEN	0.007/0.002/0.004	0.25/0.20/0.20	0.008/0.002/0.005	0.25/0.18/0.23	0.036/0.009/0.011	0.44/0.38/0.31
OH+CH ₃ OOH/ROOH	0.010/0.011/0.014	0.35/1.08/0.70	0.011/0.012/0.014	0.34/1.10/0.64	0.022/0.020/0.022	0.27/0.85/0.63
OH+ISOP	0.019/0.004/0.002	0.67/0.39/0.10	0.020/0.004/0.003	0.62/0.37/0.14	0.017/0.007/0.003	0.21/0.30/0.09
OH+PAR	0.005/0.002/0.004	0.18/0.20/0.20	0.007/0.003/0.005	0.22/0.27/0.23	0.015/0.005/0.007	0.18/0.21/0.20
OH+ONIT/ISOPRD	0.028/0.005/0.016	0.99/0.49/0.80	0.030/0.005/0.018	0.93/0.46/0.83	0.077/0.013/0.025	0.93/0.55/0.72
OH+C ₂ H ₆	0.002/0.001/0.002	0.07/0.10/0.10	0.003/0.001/0.002	0.09/0.09/0.09	0.008/0.002/0.004	0.10/0.08/0.11
OH+CH ₃ OH/ANOL/CRES	0.002/0.001/0.002	0.07/0.10/0.10	0.002/0.001/0.002	0.06/0.09/0.09	0.007/0.002/0.003	0.08/0.08/0.09
OH+HO ₂	0.001/<0.001/0.004	0.04/0.05/0.20	0.002/<0.001/0.005	0.06/0.05/0.23	0.006/<0.001/0.008	0.07/0.02/0.23
OH+NO	0.105/0.036/0.039	3.70/3.54/1.94	0.066/0.030/--	2.05/2.75/--	--/--/--	--/--/--
Total	2.839/1.017/2.009	100/100/100	3.214/1.093/2.172	100/100/100	8.261/2.360/3.495	100/100/100

820 OLET: internal olefin carbons (C=C); OLEI: terminal olefin carbons (C=C); ROOH: higher organic peroxide; ETH: ethene; ISOP: isoprene;

821 ALD2: acetaldehyde; MGLY: methylglyoxal; ANOE: acetone; XYL: xylene; TOL: toluene; HNO_x: HNO₃ + HNO₄; OPEN: aromatic fragments;

822 PAR: paraffin carbon –C–; ONIT: organic nitrate; ISOPRD: lumped intermediate species; ANOL: ethanol; CRES: cresol and higher molar

823 weight phenols.

824 *The reactions of $\text{HONO} + h\nu$, $\text{H}_2\text{O}_2 + h\nu$ and $\text{HNO}_3 + h\nu$ are reversible, “net” in the subscript means subtracting the corresponding reverse
825 reactions.
826

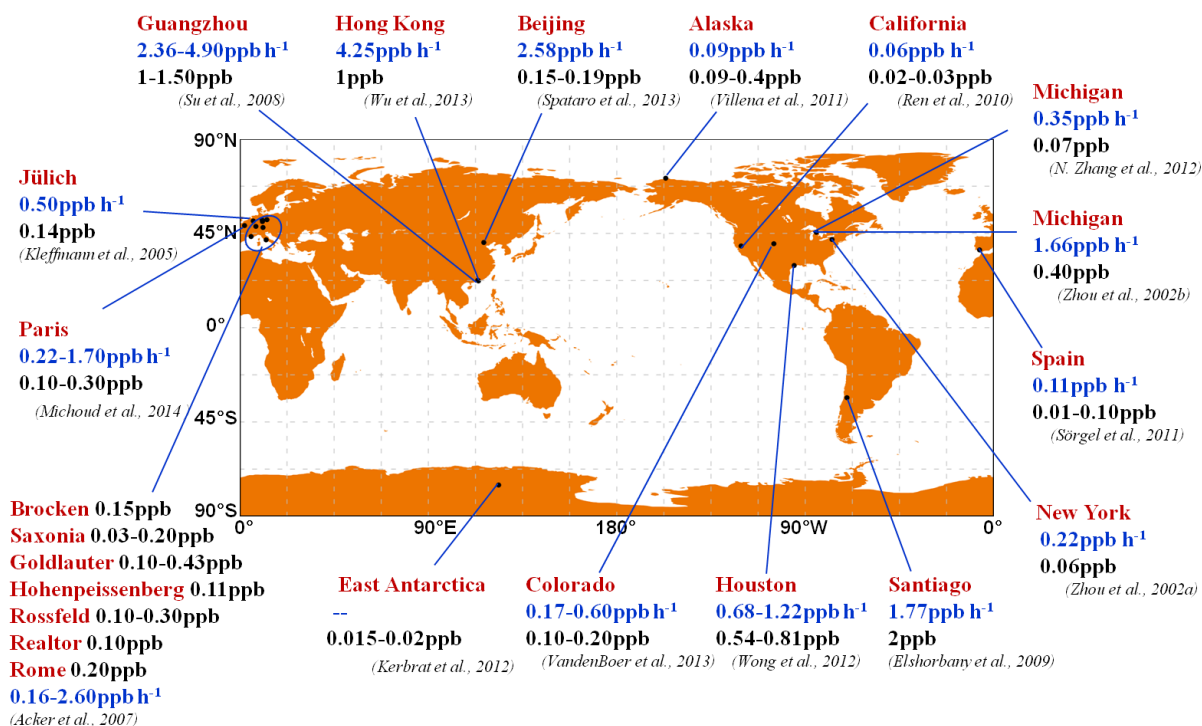


Fig. 1. Summary of observed HONO mixing ratios at noon (black font) and the calculated unknown daytime HONO source (blue font) from field studies.

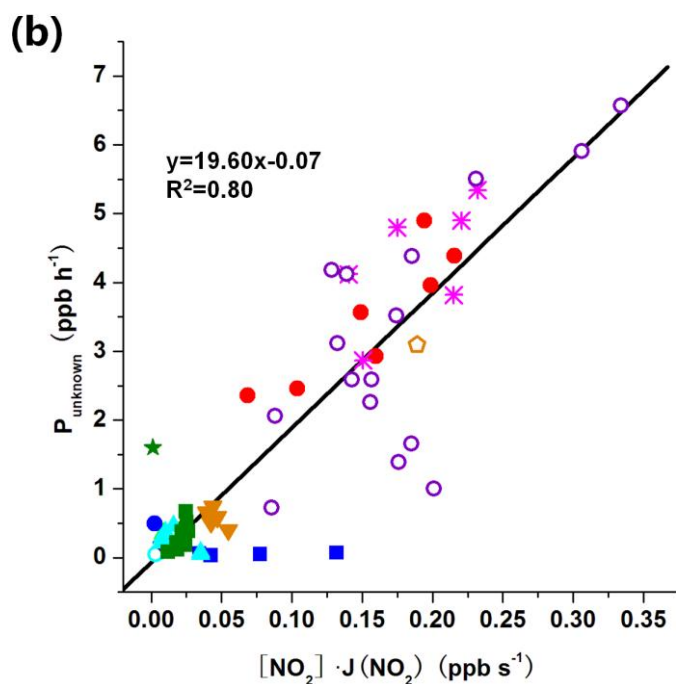
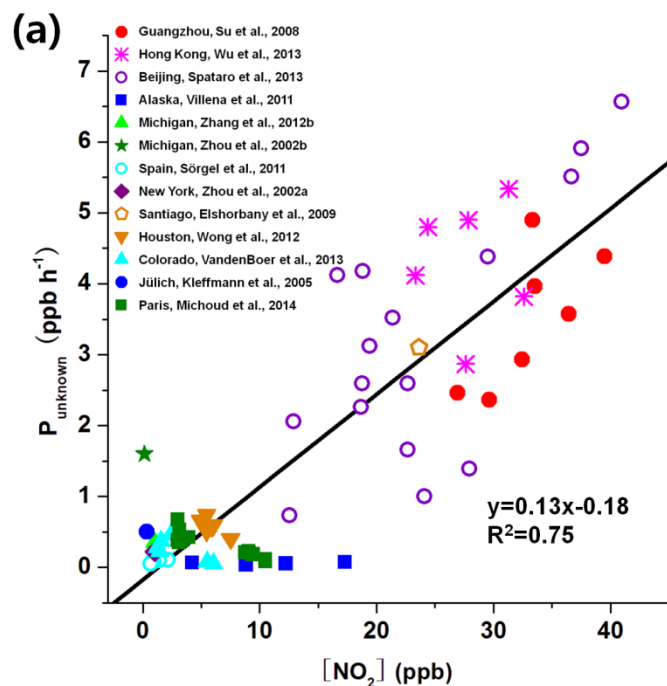


Fig. 2. Correlation of the unknown daytime HONO source (P_{unknown}) (ppb h^{-1}) with (a) $[\text{NO}_2]$ (ppb) and (b) $[\text{NO}_2] \times J(\text{NO}_2)$ (ppb s^{-1}), based on the field experiment data shown in Fig. 1.

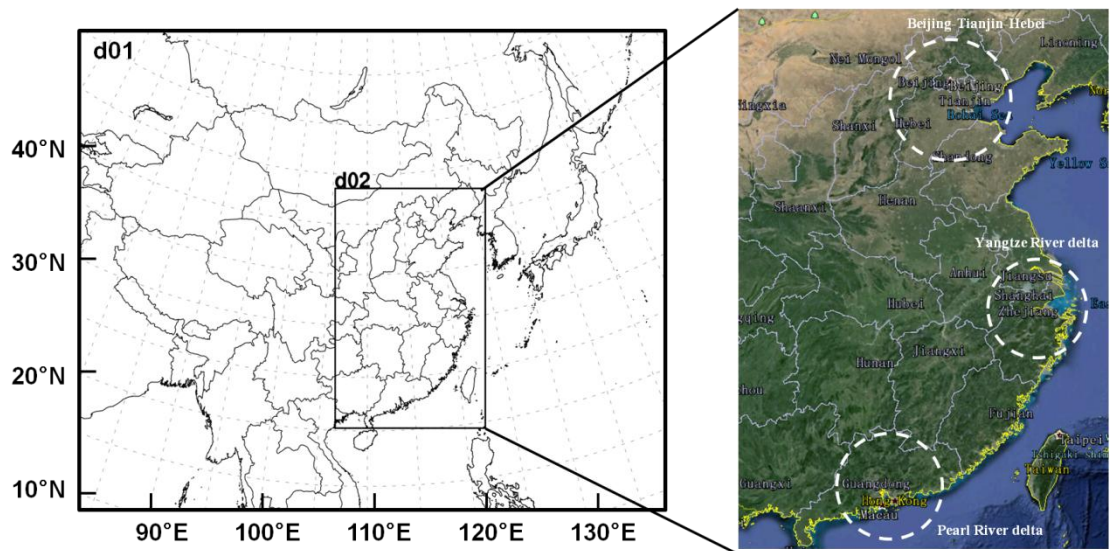


Fig. 3. Model domains used in this study. Domain 2 covers the Beijing–Tianjin–Hebei (BTH), Yangtze River delta (YRD), and Pearl River delta (PRD) regions.

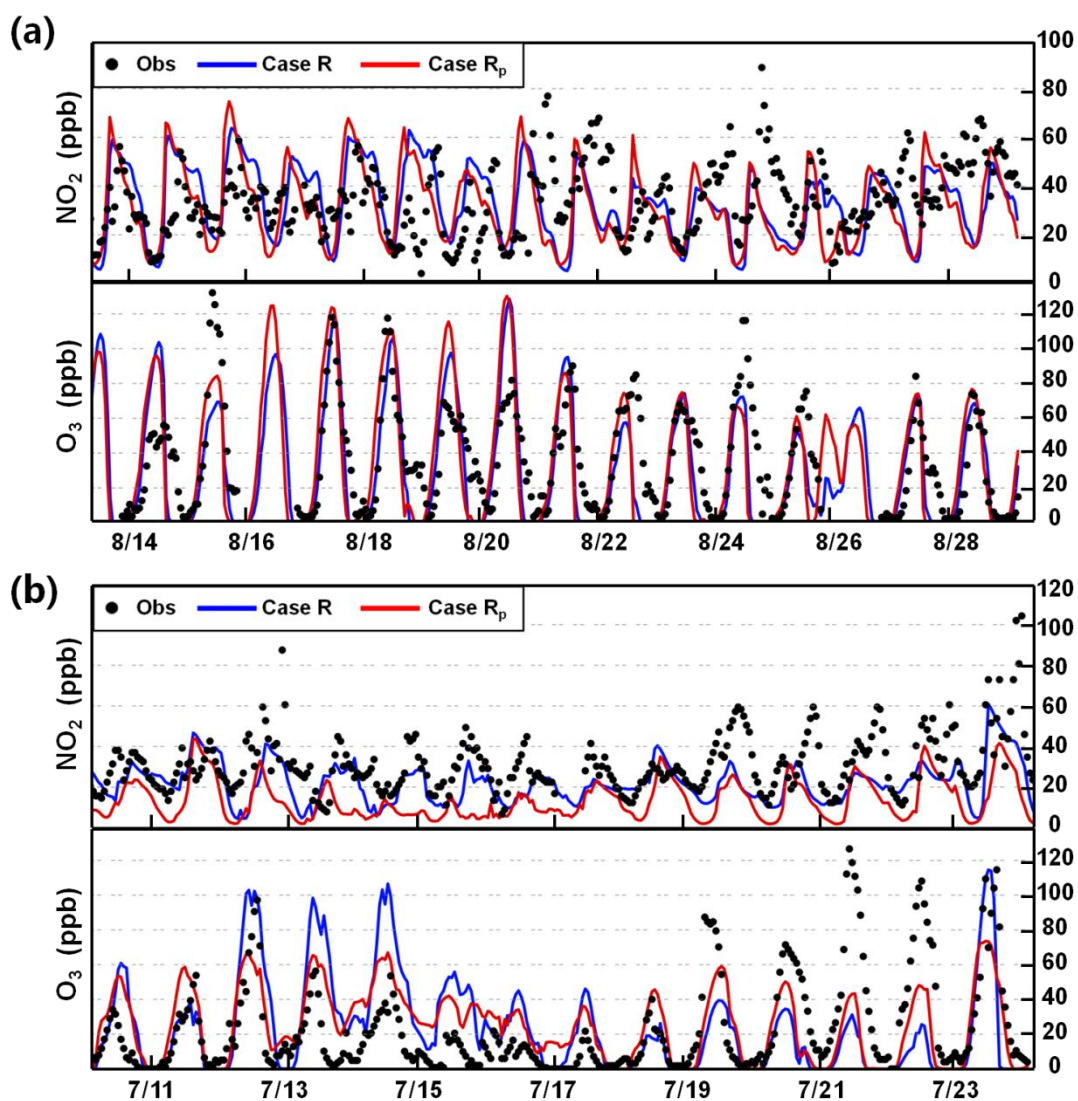


Fig. 4. Comparison of simulated and observed hourly-mean mixing ratios of NO_2 and O_3 in (a) Beijing on 14–28 August 2007 and (b) Guangzhou on 11–23 July 2006.

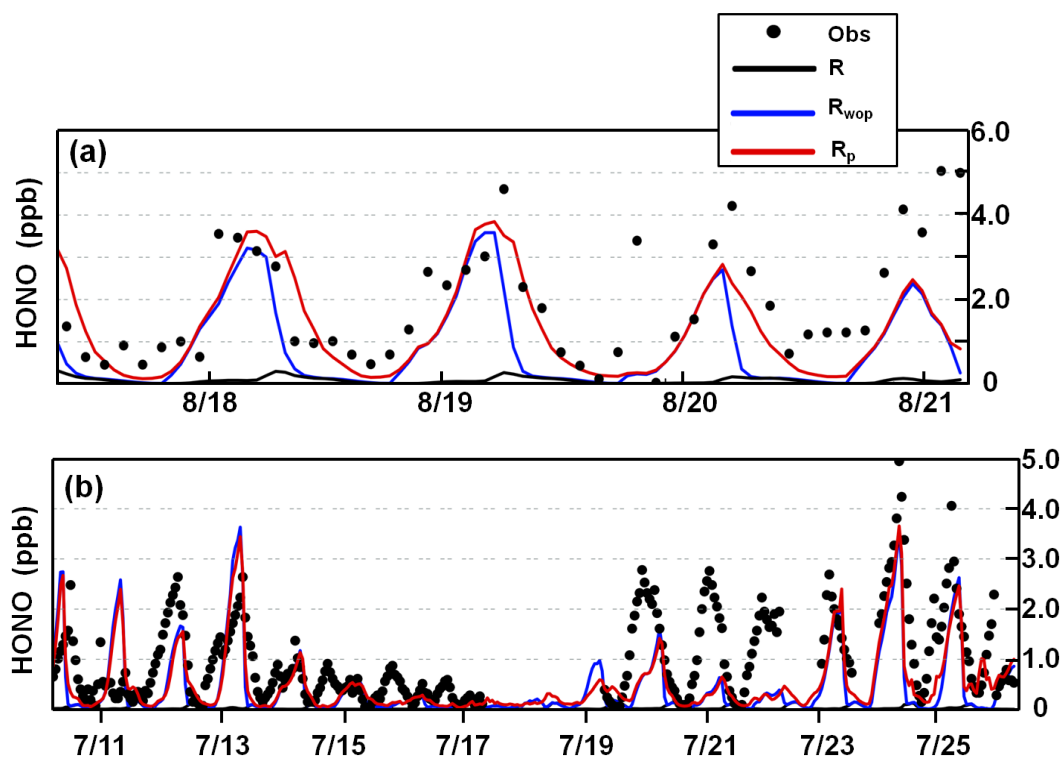


Fig. 5. Comparison of simulated and observed hourly-mean HONO mixing ratios at the Peking University site in (a) Beijing on 17–20 August 2007 (Spataro et al., 2013) and (b) the Backgarden site in Guangzhou on 11–25 July 2006 (X. Li et al., 2012).

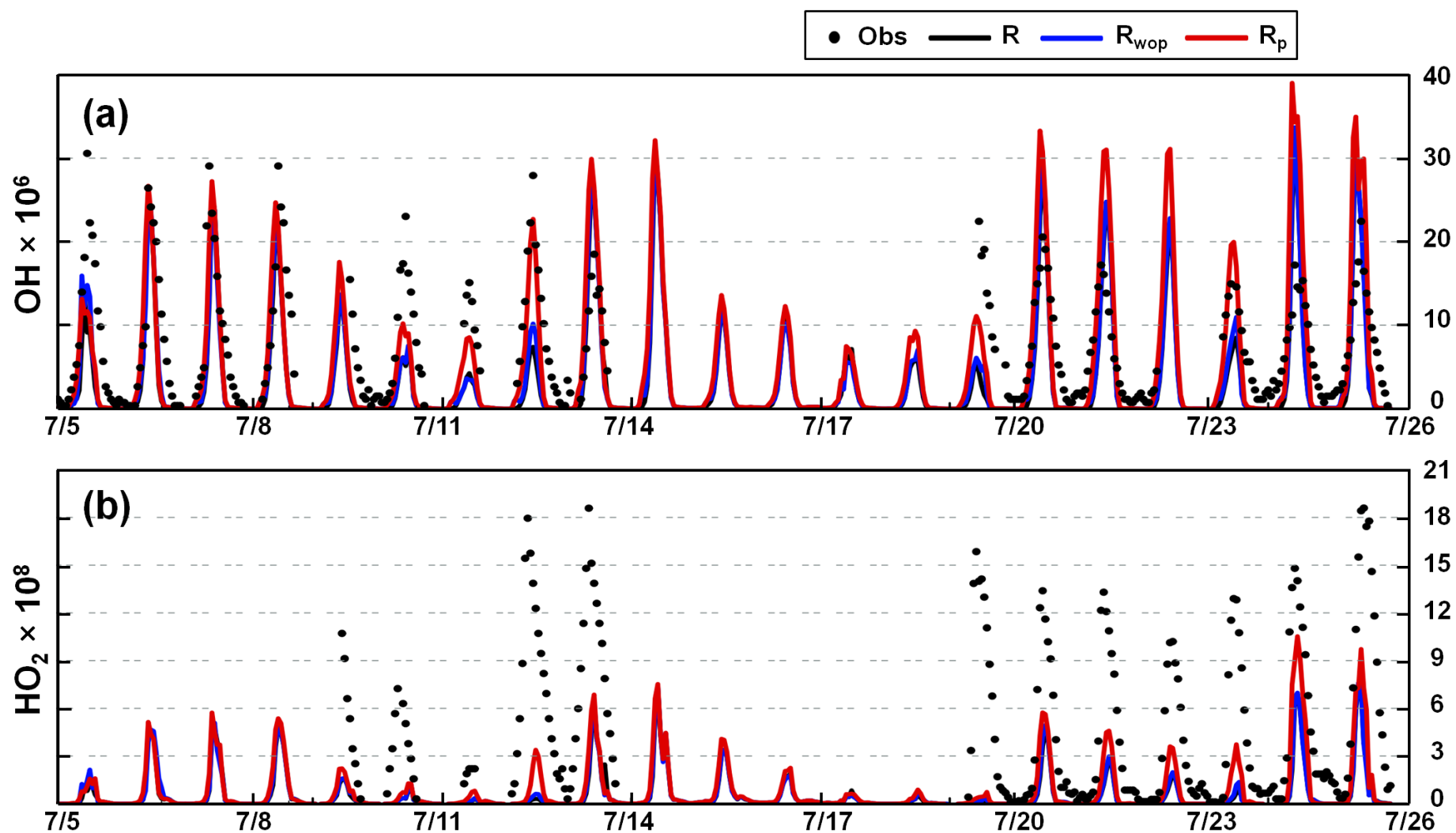


Fig. 6. Comparison of simulated and observed hourly-mean mixing ratios of OH and HO₂ at the Backgarden site in Guangzhou in July 2006 (Lu

897 et al., 2012).

898

899

900

901

902

903

904

905

906

907

908

909

910

911

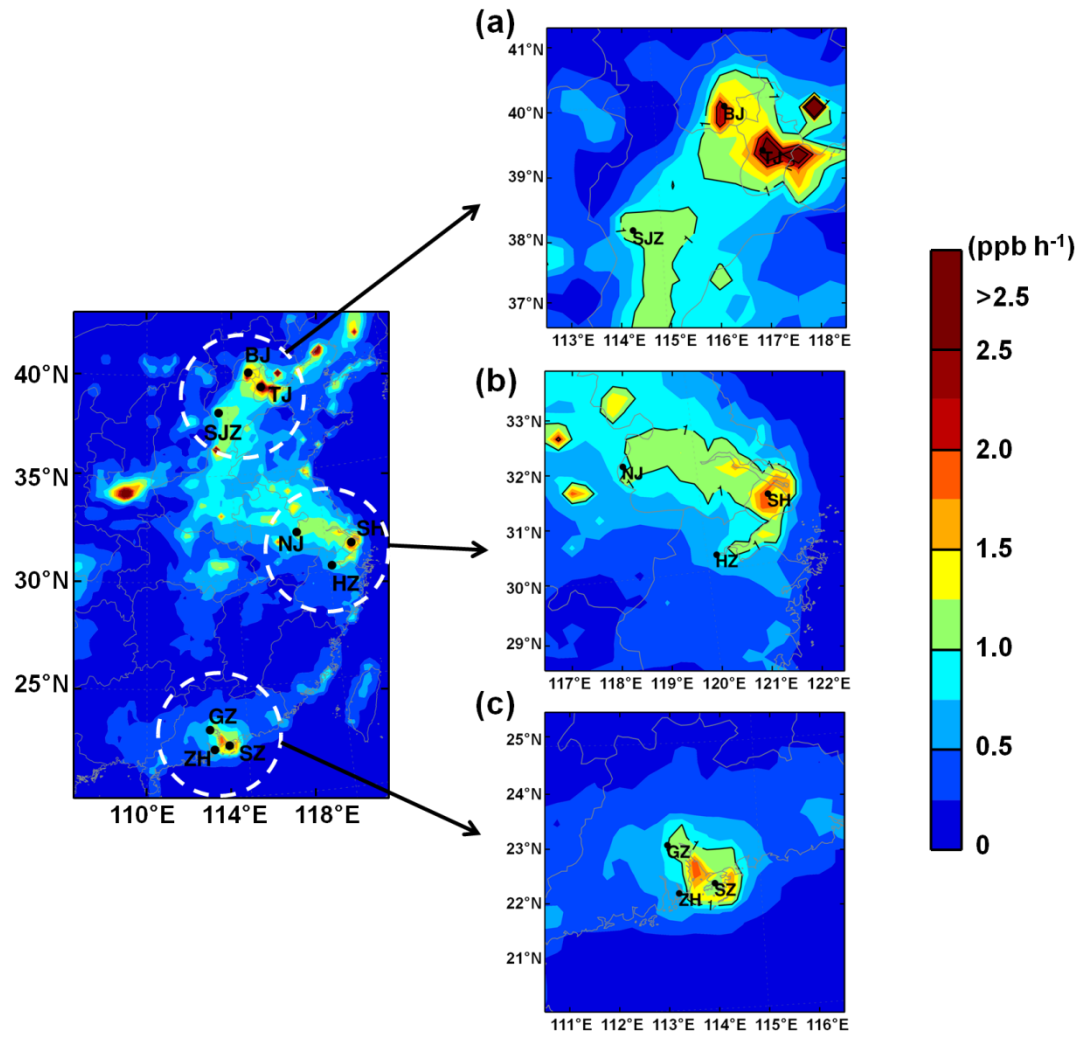


Fig. 7. Simulated unknown daytime HONO source (ppb h^{-1}) in the (a) BTH, (b) YRD, and (c) PRD regions in August 2007 (BJ, Beijing; TJ, Tianjin; SJZ, Shijiazhuang; SH, Shanghai; NJ, Nanjing; HZ, Hangzhou; GZ, Guangzhou; ZH, Zhuhai; SZ, Shenzhen).

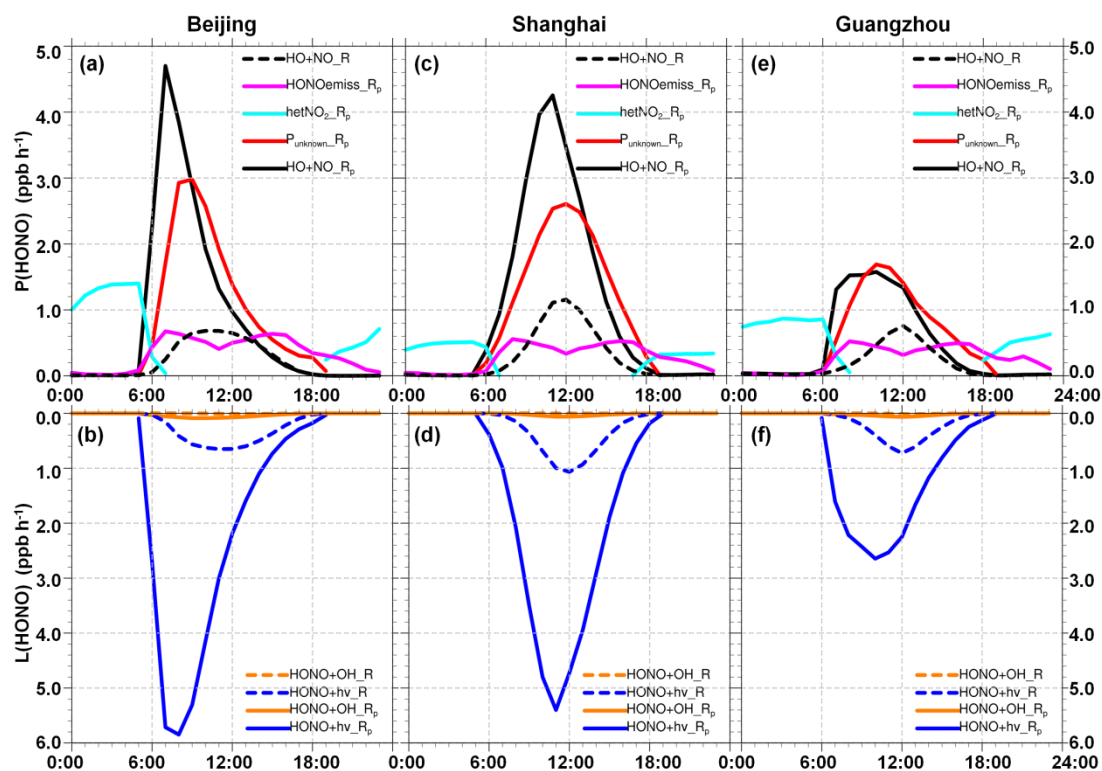


Fig. 8. Production [P(HONO)] and loss [L(HONO)] rates of HONO for cases R (dashed lines) and R_p (solid lines) in (a, b) Beijing, (c, d) Shanghai, and (e, f) Guangzhou in August 2007.

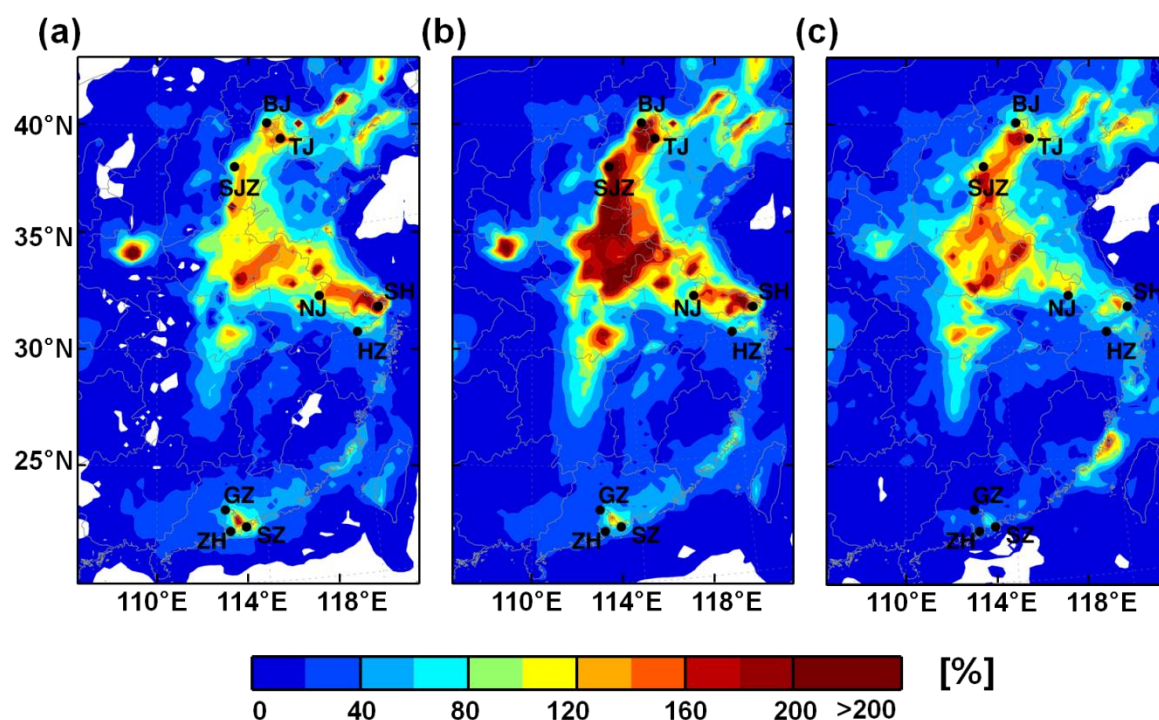


Fig. 9. Daytime (06:00–18:00 LST) percentage enhancements of (a) OH, (b) HO₂, and (c) RO₂ due to the unknown daytime HONO source (case R_p – case R_{wop}) in the coastal regions of China in August 2007.

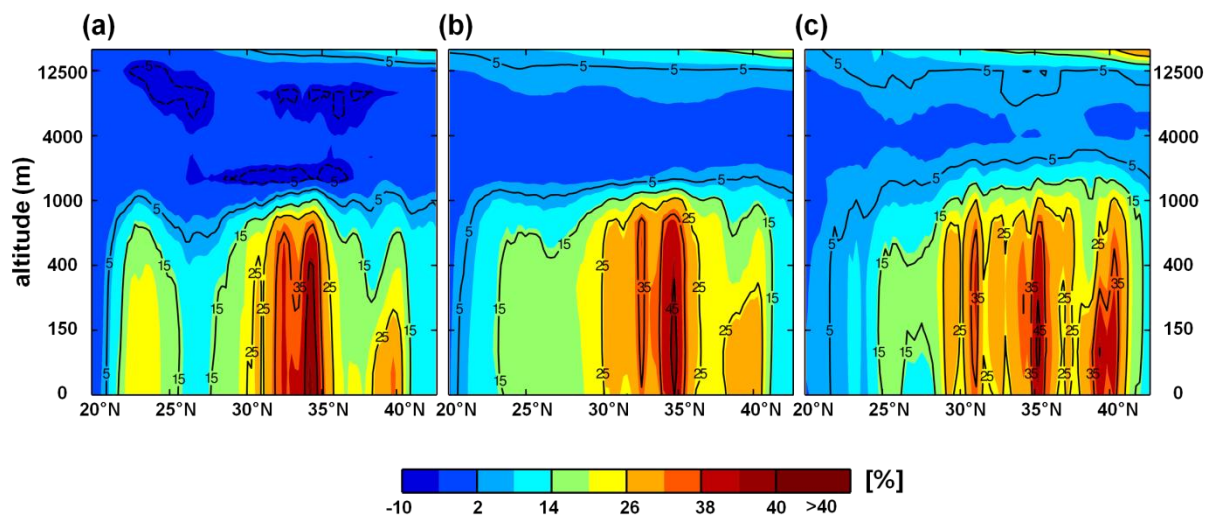


Fig. 10. Daytime (06:00–18:00 LST) meridional-mean percentage enhancements of (a) OH, (b) HO₂, and (c) RO₂ due to the unknown daytime HONO source (case R_p – case R_{wop}) in the coastal regions of China in August 2007.

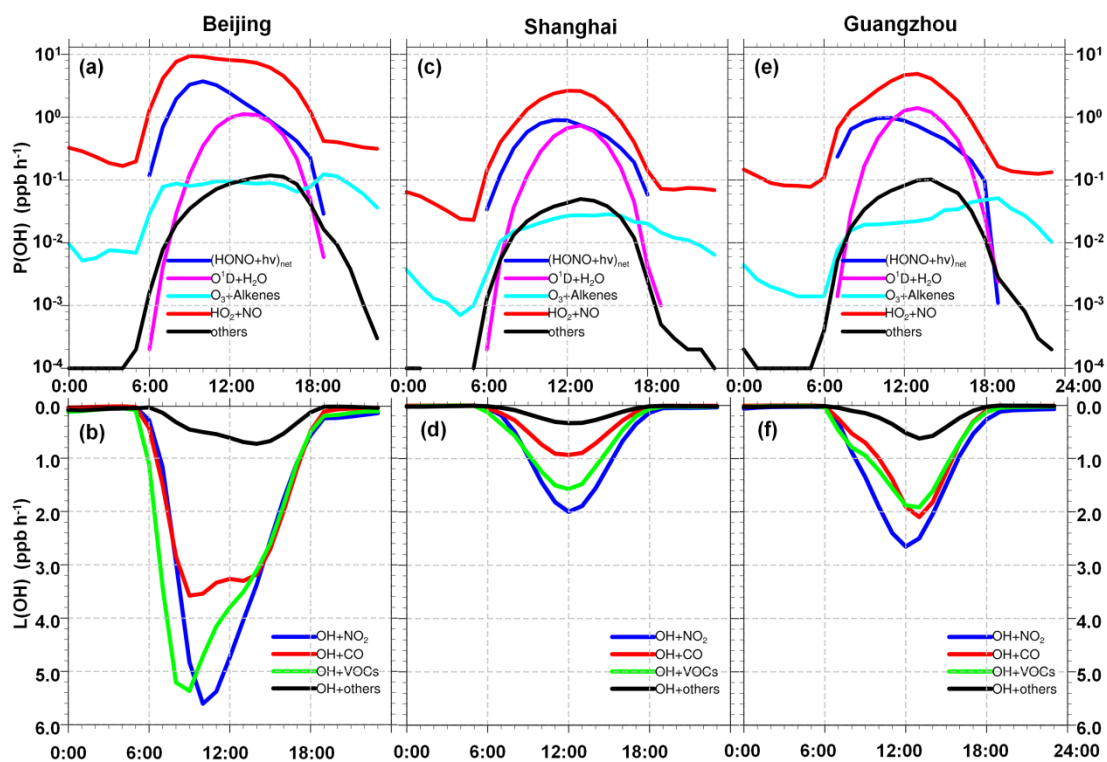


Fig. 11. Averaged production $[P(OH)]$ and loss $[L(OH)]$ rates of OH for case R_p in (a, b) Beijing, (c, d) Shanghai, and (e, f) Guangzhou in August 2007. $(HONO+h\nu)_{net}$ means the net OH production rate from HONO photolysis (subtracting $OH + NO = HONO$).

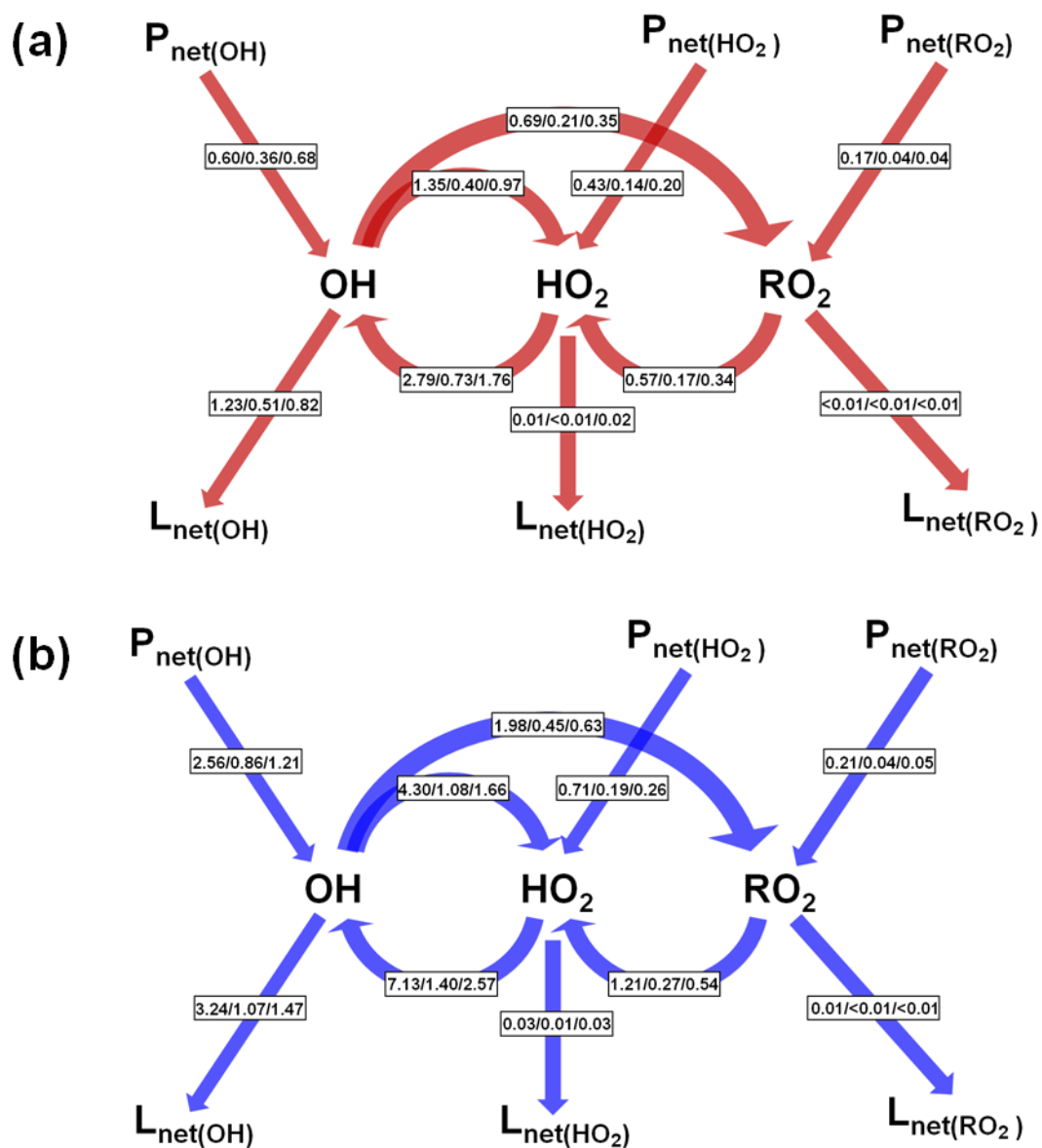


Fig. 12. Daytime (06:00–18:00 LST) average budgets of OH, HO₂ and RO₂ radicals (reaction rates, ppb h⁻¹) for cases (a) R and (b) R_p in Beijing/Shanghai/Guangzhou in August 2007.

